GPR55 regulates the responsiveness to, but does not dimerise with, α1A-adrenoceptors.

WALSH, S.K., LIPINA, C., ANG, S.Y., SATO, M., CHIA, L.Y., KOCAN, M., HUTCHINSON, D.S., SUMMERS, R.J. and WAINWRIGHT, C.L.

2021

Title: GPR55 regulates the responsiveness to, but does not dimerise with, α_{1A}-adrenoceptors

Sarah K Walsh[1*], Christopher Lipina[2], Sheng Y Ang[3], Masaaki Sato[3], Ling Yeong Chia[3], Martina Kocan[4], Dana S Hutchinson[3], Roger J Summers[3], Cherry L Wainwright[1]

Author Affiliations

[1]Cardiometabolic Health Research, School of Pharmacy and Life Sciences, Robert Gordon University, Sir Ian Wood Building, Aberdeen, AB10 7GJ, UK

[2]Division of Cell Signalling and Immunology, Sir James Black Centre, School of Life Sciences, University of Dundee, Dundee, DD1 5EH, UK

[3]Drug Discovery Biology, Monash Institute of Pharmaceutical Sciences, Monash University, Parkville, VIC, Australia

[4]The Florey Institute of Neuroscience and Mental Health and School of Biosciences, University of Melbourne, Parkville, VIC, Australia

[*]**Corresponding author:** Dr Sarah K Walsh, Cardiometabolic Health Research, School of Pharmacy and Life Sciences, Robert Gordon University, Sir Ian Wood Building, Garthdee Road, Aberdeen, AB10 7GJ, UK. Email: s.walsh@rgu.ac.uk Tel: (0)1224 262562

Category: Cardiovascular Pharmacology

Abstract

Emerging evidence suggests that G protein coupled receptor 55 (GPR55) may influence adrenoceptor function/activity in the cardiovascular system. Whether this reflects direct interaction (dimerization) between receptors or signalling crosstalk has not been investigated. This study explored the interaction between GPR55 and the alpha 1A adrenoceptor (α_{1A}-AR) in the cardiovascular system and the potential to influence function/signalling activities. GPR55 and α_{1A}-AR mediated changes in both cardiac and vascular function was assessed in male wild-type (WT) and GPR55 homozygous knockout ($GPR55^{-/-}$) mice by pressure volume loop analysis and isolated vessel myography, respectively. Dimerization of GPR55 with the α_{1A}-AR was examined in transfected Chinese hamster ovary-K1 (CHO-K1) cells via Bioluminescence Resonance Energy Transfer (BRET). GPR55 and α_{1A}-AR mediated signalling (extracellular signal-regulated kinase 1/2 (ERK1/2) phosphorylation) was investigated in neonatal rat ventricular cardiomyocytes using AlphaScreen proximity assays. $GPR55^{-/-}$ mice exhibited both enhanced pressor and inotropic responses to A61603 (α_{1A}-AR agonist), while in isolated vessels, A61603 induced vasoconstriction was attenuated by a GPR55-dependent mechanism. Conversely, GPR55-mediated vasorelaxation was not altered by pharmacological blockade of α_{1A}-ARs with tamsulosin. While cellular studies demonstrated that GPR55 and α_{1A}-AR failed to dimerize, pharmacological blockade of GPR55 altered α_{1A}-AR mediated signalling and reduced ERK1/2 phosphorylation. Taken together, this study provides evidence that GPR55 and α_{1A}-AR do not dimerize to form heteromers, but do interact at the signalling level to modulate the function of α_{1A}-AR in the cardiovascular system.

Key words: GPR55; α_{1A}-adrenoceptor; cardiac function; receptor crosstalk

1. Introduction

G protein coupled receptor 55 (GPR55) is a rhodopsin-like seven transmembrane/G protein-coupled receptor [1] with the phospholipid lysophosphatidylinositol (LPI) suggested as the endogenous ligand [2]. GPR55 is widely expressed in humans [3] and rodents [4], and within the cardiovascular system is present in vascular smooth muscle and endothelial cells [5] and in ventricular cardiomyocytes [6]. Functionally, GPR55 activation by LPI induces a vasodilator response in isolated blood vessels [7], and both depolarization (via an inositol triphosphate (IP_3)/Ca^{2+} induced Ca^{2+} release/L-type Ca^{2+} channel; LTCC) and hyperpolarization in cardiomyocytes, through receptors located in the sarcolemmal and endo-lysosomal compartments, respectively [8]. Additionally, the GPR55 antagonist cannabidiol (CBD) attenuates excitation-contraction coupling in ventricular cardiomyocytes by inhibition of LTCC channels [9]. Beyond this, little is known regarding the role of GPR55 in the physiological control of the cardiovascular system.

We previously demonstrated that lack of GPR55 ($GPR55^{-/-}$ mice) does not affect basal systolic or diastolic function in young mice, suggesting that it does not play a direct role in the control of cardiac contractility. However, these mice did exhibit cardiac decompensation following adrenoceptor stimulation with dobutamine [6]. Thus, GPR55 may play a pivotal role in regulating the activity of other GPCRs responsible for maintaining cardiac function. Indeed, there is increasing evidence that GPR55 influences/regulates the downstream signalling of, and forms heteromers with, other GPCRs, notably both cannabinoid 1 (CB_1) [10,11] and cannabinoid 2 (CB_2) receptors [12,13].

Dobutamine is an agonist at β_1-, β_2- and α_1-adrenoceptors (β_1-AR, β_2-AR and α_1-AR), all of which contribute to its inotropic action [14]. α_{1A}-ARs contribute ~25% to the inotropic response to noradrenaline [15] and selective α_1-AR activation induces robust positive inotropic responses in the hearts of rats [16], humans [17], and other experimental animals *in vivo* [18]. Thus, our findings that inotropic responses to dobutamine in GPR55$^{-/-}$ mice are diminished [6] may reflect alterations in either β_1-AR or α_1-AR signalling, or both. Like GPR55, α_{1A}-ARs have been reported to form heteromers with other receptors, such as the chemokine receptor 4 [19,20] and endothelin A receptor [21] that can either regulate or sensitise (by allosteric modulation) downstream responses to α_{1A}-AR activation. Although formation of GPR55/α_{1A}-AR heteromers has yet to be demonstrated, both receptor types are localised in cardiovascular cells [5]. In addition, LPI-induced activation of a CBD-sensitive receptor (most likely GPR55) prevents noradrenaline-induced vasoconstriction [22], while chronic antagonism of α_{1A}-ARs increased GPR55 expression in a cancer cell line [23]. Taken together this implies interaction between GPR55 and α_1-ARs, that may go some way to explaining reduced inotropic responses to AR activation in GPR55$^{-/-}$ mice. The present study was therefore designed to determine the effect of GPR55 deletion on inotropic and vasoconstrictor responses to α_{1A}-AR activation, and on α_{1A}-AR expression. We then examined whether changes in functional responses could be explained by heteromerization/crosstalk between GPR55 and α_{1A}-ARs.

2. Materials and Methods

2.1. Animal housing and ethical approval

Homozygous GPR55 knockout (GPR55$^{-/-}$) mice were bred from our existing colony and C57Bl/6 (wild-type; WT) mice were supplied by the University of Aberdeen Medical

Research Facility, where both strains were housed at a temperature of 21±2°C, with a 12 hr light/dark cycle and free access to food and tap water. As published data indicates that gender differentially affects the responsiveness of adrenoceptors in the cardiovascular system [24,25] only one gender (male mice) was used for experimental studies examining adrenoceptor mediated responses *in vivo* and in isolated blood vessels. Animals were transferred to the Biological Services Unit at Robert Gordon University on a weekly basis and allowed to acclimatize for 24 hours before commencing the study. The welfare of all transported animals was assessed by trained staff prior to undergoing *in vivo* experimentation and none were required to be excluded. All studies were performed under an appropriate Project License authorized under the UK Animals (Scientific Procedures) Act 1986 and conform to the guidelines from Directive 2010/63/EU of the European Parliament on the protection of animals used for scientific purposes. Pregnant Sprague-Dawley rats (14-18 days gestation) were obtained from Monash University Animal Research Platform (MARP; Clayton, VIC, Australia) and transported to Monash Institute of Pharmaceutical Sciences (MIPS; Parkville, VIC, Australia), where they were acclimatised for 4-8 days prior to littering. New-born rats were used for the generation of cardiomyocytes at 0-3 days post birth. Experiments complied with the Australian code for the care and use of animals for scientific purposes (National Health and Medical Council of Australia, 8th edition), and experiments were reviewed and approved by the Monash University Animal Ethics Committee (Australia; ethics number MIPS.2015.14). All *in vivo* work is reported in accordance with the ARRIVE guidelines [26].

2.2. Pressure volume loop analysis

Four month old male WT (29±0.5g) and GPR55$^{-/-}$ (28±0.5g) mice were anaesthetised with a mixture of ketamine (120mg kg^{-1}; Vetalar; Pfizer, Dublin, Ireland) and xylazine (16mg kg^{-1}; Rompun; Bayer, Dublin, Ireland) via intraperitoneal (i.p.) injection. The right jugular vein was cannulated with flame-stretched Portex polythene tubing (0.58mm ID x 0.96mm OD; Smiths Medical International Ltd., Hyde, Kent, UK) for drug administration. Ventricular function was measured in closed-chest mice via pressure volume analysis using a method adapted from Pacher et al. [27]. Briefly, the neck was opened, the right carotid artery isolated, and a 1.4-Fr pressure conductance catheter (SPR-839; Millar Inc., Houston, TX, USA) inserted into the vessel. Baseline arterial pressure (systolic (SBP), diastolic (DBP), and mean arterial blood pressure (MABP)) was measured prior to the advancement of the catheter into the left ventricle for the recording of cardiac function via the MPVS-Ultra Single Segment Foundation System (Millar Inc., Houston, TX, USA). A steel thermistor probe (Fisher Scientific UK Ltd., Loughborough, Leicestershire, UK) was inserted into the rectum to measure core temperature, which was maintained at 37-38^{o}C with the aid of a Vetcare heated pad (Harvard Apparatus Ltd., Cambourne, Cambridge, UK). Anaesthesia was maintained throughout by administration of 50µL per 25g (body weight) of the ketamine and xylazine mixture via i.p. injection every 40 min or as required. Post stabilisation, baseline cardiac function was recorded in all mice and then pharmacological agents administered via an intravenous (i.v.) bolus dose to both WT and GPR55$^{-/-}$ mice and the change from baseline function calculated. To examine the effect of GPR55 activation on cardiac function, LPI (10-100µg kg^{-1} i.v.; GPR55 agonist; Sigma-Aldrich, St Louis, MO, USA), was administered to WT mice (n=8) in non-cumulative incremental doses. To examine the influence of GPR55 presence on α_{1A}-AR mediated functional

changes, both WT and GPR55$^{-/-}$ mice (n=9 for each strain) were administered the α_{1A}-AR agonist, A61603 (0.2-20μg kg^{-1} i.v.; Sigma-Aldrich, Saint Louis, MO, USA) [28], absence or the presence (highest concentration of A61603 (20μg kg^{-1}) only) the selective α_1-AR antagonist, prazosin (1mg kg^{-1} i.p.) [29,30]. In a separate series of studies, both male WT and GPR55$^{-/-}$ mice (age-matched to those used for the measurement of cardiovascular function; n=6-10) were euthanised via an overdose of anaesthetic (150mg kg^{-1} i.p.; Pentobarbital sodium; Euthatal®; Boehringer Ingelheim Animal Health, Woking, UK.), the heart removed, ventricular tissue separated, and flash frozen in liquid nitrogen for the determination of both mRNA (qRT-PCR) and protein (immunoblot analysis) expression of α_{1A}-ARs. Carotid arteries were also collected from these animals for the assessment of vascular function via isometric myography. Experimental group sizes for both haemodynamic measurements and vascular function were chosen on the basis of previously published literature examining similar end-points [31,32].

2.3. Isometric myography

Carotid arteries from WT and GPR55$^{-/-}$ mice were cleaned of perivascular fat and mounted onto a two-channel wire myograph (Model 510A, Danish Myo Technology (DMT), Aarhus, Denmark) containing oxygenated (95% O_2 & 5% CO_2) Krebs Henseleit buffer (119mM NaCl, 4.7mM KCl, 1.18mM KH_2PO_4, 2.41mM $MgSO_4$, 25mM $NaHCO_3$, 2.52mM $CaCl_2$ and 10.88mM glucose; pH7.4; all chemicals were purchased from Fisher Scientific UK Ltd., Loughborough, Leicestershire, UK) at 37^{o}C. Vessels were normalised to achieve a transmural pressure of 100mmHg using the DMT Normalisation software. Isometric tension was recorded and displayed using a PowerLab and Chart Software (both AD Instruments, Cowley, Oxfordshire, UK). The

viability of the smooth muscle was tested via the addition of an 80mM KCl solution. To determine the influence of GPR55 receptors on α_{1A}-AR-mediated vasoconstriction, cumulative concentration response curves were constructed for A61603 (10^{-10}-10^{-5}M) in the absence and presence of the GPR55 antagonist, CID16020046 (30 or 100μM; Sigma-Aldrich, St Louis, MO, USA) [33], in arteries from both strains of mice; tamsulosin (10nM) was used to confirm that A61603 was acting via α_{1A}-ARs. In a separate series of experiments, to determine the influence of α_{1A}-ARs on the vasodilator response to LPI, vessels were precontracted with a submaximal concentration (EC_{80}; 300nM) of the thromboxane mimetic, 9,11-Dideoxy-11α,9α-epoxymethanoprostaglandin F2α (U46619; Enzo Life Sciences (UK) Ltd., Exeter, Devon, UK), and cumulative concentration response curves carried out with LPI in the absence and presence of CID16020046 (30 or 100μM) or tamsulosin (10nM; Sigma-Aldrich, St Louis, MO, USA).

2.4. RNA isolation and Quantitative Reverse Transcription PCR (qRT-PCR) analysis (Ventricular tissue)

Briefly, frozen heart tissue was ground in a mortar in liquid nitrogen. Tri-Reagent® (Sigma-Aldrich, St Louis, MO, USA) was immediately added to the frozen powdered sample and total RNA extracted according to manufacturer's instructions. Genomic DNA was removed by RNase-free DNase I (New England Biolabs (UK) Ltd., Hitchin, Hertfordshire, UK) treatment at 37°C for 10 min following the protocol provided by the manufacturer. Total RNA concentrations were measured using UV absorbance spectrophotometry. Purity of RNA was checked by determining the ratio of absorbance readings at 260nm and 280nm. RNA purity of samples included in subsequent analysis was considered adequate when the A260/A280 ratio was $\geq$1.8. Reverse transcription

(as per one reaction) was performed at 42°C for 1 hr using 200U of Moloney murine leukemia virus reverse transcriptase (Promega, Southampton, Hampshire, UK), 1µg of total RNA and 0.5µg oligo $(dT)_{18}$ primer according to manufacturer's instructions. qRT-PCR was performed using a StepOne Plus Real-Time PCR System (Applied Biosystems, Foster City, CA, USA) and SYBR Green JumpStart Taq Ready Mix (Sigma-Aldrich, St Louis, MO, USA). 18S rRNA (18S ribosomal ribonucleic acid) was amplified as an internal control. The mouse sequences for primers used (designed from GenBank (http://www.ncbi.nlm.nih.gov/) with the aid of the National Center for Biotechnology Information Primer-BLAST design tool) were as follows: α_{1A}-AR (sense: CAGATGGAGTCCGTGAATGGAA & antisense: AATGGTTGGAACTTGGTGATTT) and 18S rRNA (sense: CAGCCACCCGAGATTGAGCA & antisense: TAGTAGCGACGGGCGGTGTG). All qRT-PCR amplifications were performed with an initial denaturation step at 95°C for 10 min followed by 40 cycles of denaturation at 95°C for 15s, annealing at 55°C for 15s, and extension at 68°C for 1 min. The ratio of target mRNA to 18S rRNA mRNA was calculated using a mathematical model previously described [34]. A negative control (deionised H_2O) was included for each qRT-PCR run. Measurements of gene expression were performed in triplicate for each RNA sample and a mean value used for further analysis.

2.5. Protein Extraction, SDS-PAGE and Immunoblotting

For total protein extraction, frozen heart tissue was ground using a pestle and mortar prior to homogenization with ice cold lysis buffer (50mM Tris/HCl pH 7.4, 0.27M sucrose, 1mM sodium orthovanadate, 1mM EDTA, 1mM EGTA, 10mM sodium 2-glycerophosphate, 50mM sodium fluoride, 5mM sodium pyrophosphate, 1% (v/v) Triton X-100, 0.1% (v/v) 2-mercaptoethanol and protease inhibitor (one tablet/50 ml);

all purchased from Sigma-Aldrich, St Louis, MO, USA). Cell/tissue debris was removed from crude lysates by centrifugation at 3000*g* for 10 min at 4°C, and the resulting supernatant used for Western blot analysis. Total protein extracts (30µg) were fractionated by SDS-polyacrylamide gel electrophoresis and immunoblotted using anti-actin (Sigma-Aldrich, Dorset, UK) and anti-α_{1A}-AR (ab137123; Abcam, Cambridge, Cambridgeshire, UK) antibodies as previously described [35]. Primary antibody detection was carried out using a horseradish peroxidase-conjugated anti-rabbit or anti-mouse IgG antibody (New England Biolabs (UK) Ltd., Hitchin, Hertfordshire, UK), and visualised by enhanced chemiluminescence. Resulting band intensities were quantified using ImageJ software (National Institutes of Health, Bethesda, MD, USA).

2.6. Bioluminescence resonance energy transfer (BRET) Studies

BRET saturation curves were carried out using Chinese hamster ovary (CHO-K1) cells (obtained from American Type Culture Collection (ATCC)) co-transfected with cDNA constructs encoding α_{1A}-AR-Rluc8 (donor) and either GPR55-Venus (acceptor) or vasopressin 2 receptor (V2R)-Venus (used as a positive control in the present study as it has previously been shown to dimerise with α_{1A}-AR [36]). Human α_{1A}-AR sequence was amplified from the cDNA clone described in [37], purified using the Ultraclean 15 DNA purification kit (Qiagen Pty Ltd., Chadstone, VIC 3148, Australia) and cloned into pDONR201 with BP clonase II (both from (Thermo Fisher Scientific Inc., Waltham, MA, USA) at 25°C for 16 h. Rluc8 cDNA was amplified, purified and cloned into pEF5/FRT/V5−DEST vector [38]. An expression clone of α_{1A}-AR-Rluc8 was created using LR clonase at 25°C for 16 h. The preparation of V2R-Venus cDNA construct has been described previously [39]. For generation of GPR55-Venus, Human GPR55 sequence was first amplified by PCR from pcDNA3.1+ containing GPR55

using the forward primer 5′-GGGGACAAGTTTGTACAAAAAAGCAGGCTACCATGAGTCAGCAAAACACCAGTG-3′ (start codon underlined) and reverse primer 5′-GGGGACCACTTTGTACAAGAAAGCTGGGTCGCCCCGGGAGATCGTGGTGTCCTGC-3′, containing attB1 and attB2 sites respectively. The PCR product was purified from gel and cloned into pDONR201 vector using BP clonase II to create an entry clone containing attL1- and attL2-flanked GPR55 sequence. An LR recombination reaction was performed between the entry clone and the pEF5/FRT/V5−DEST vector containing the Venus insert to create a Venus-tagged GPR55 at the C-terminus (GPR55-Venus). All construct sequences were confirmed by DNA sequencing at the Australian Genome Research Facility (Melbourne, Australia). Prior to transient transfection, CHO-K1 cells were seeded in a 6-well plate (250,000 cells/well) in Dulbecco's Modified Eagle Medium (DMEM) containing 4.5g/L D-glucose, 0.11g/L sodium pyruvate and 4mM L-glutamine (supplemented with 5% foetal bovine serum (FBS)) (all from Thermo Fisher Scientific Inc., Waltham, MA, USA) and cultured overnight in 5% CO_2 at 37ºC. DMEM medium was then replaced with Opti-MEM medium (containing HEPES, 2.4g/L sodium bicarbonate and L-glutamine; Thermo Fisher Scientific Inc., Waltham, MA, USA) and cells co-transfected with cDNA constructs encoding α_{1A}-AR-Rluc8 (250ng) and increasing amounts (0-1750ng) of either GPR55-Venus or V2R-Venus using Lipofectamine™ 2000 (Thermo Fisher Scientific Inc., Waltham, MA, USA) as per the manufacturer's instructions. Following 24hr, transfected cells were harvested and then seeded in 96-well plates (50,000-60,000 cells/well) in phenol red free DMEM (containing 4.5g/L D-glucose, 4mM L-glutamine and 25mM HEPES; Thermo Fisher Scientific Inc., Waltham, MA, USA) for subsequent BRET analysis. To calculate the Venus/Rluc8 ratio (acceptor signal/donor

signal) both the donor and acceptor fluorescence (excitation 500nm; emission 535nm) were measured with the use of a multi-label plate reader (EnVision 2103; PerkinElmer, Waltham, MA, USA). BRET measurements were taken at 37°C using the LUMIstar Omega plate reader (BMG Labtech, Ortenberg, Germany). Dual light emission (donor wavelength 400-475nm; acceptor wavelength 520-540nm) was simultaneously recorded and the BRET ratio (acceptor signal/donor signal) calculated and plotted against the Venus/Rluc8 ratio. In each experiment three replicates were included to generate one data point and three or more independent experiments were carried out.

2.7. RNA isolation and qRT-PCR analysis (Neonatal rat ventricular cardiomyocytes)

Hearts from 0-3-day-old Sprague Dawley rats were removed under aseptic conditions, the ventricles dissected and incubated with 0.1% trypsin (Life Technologies, NY, USA) in Hanks balanced salt solution (Sigma-Aldrich, St Louis, MO, USA) at 4ºC overnight with mixing. Trypsin was deactivated with DMEM supplemented with 10% FBS and cells dissociated with type II collagenase treatment (2.5 mg/ventricle; Worthington Biochemical Corp., Lakewood, NJ, USA) at 37ºC in a shaking incubator for 10 min at 100 rpm, a total of four times. At the end of digestion period, the dispersed cells were centrifuged for 5 min at 400g and resuspended in DMEM containing 10% FBS. Cells were pre-plated on 150mm culture dishes for 1 hr at 37ºC to remove fibroblasts. Nonadherent cells (myocytes) were transferred to another dish for another 1 h of pre-plating, before being plated in 6 well plates in DMEM containing 10% FBS, 0.11g/L sodium pyruvate, 100U/ml penicillin, 100µg/ml streptomycin and 100mM 5-Bromo-2-deoxyuridine (BrdU; Sigma-Aldrich, St Louis, MO, USA) overnight to reduce the proportion of proliferative cardiac fibroblasts. Media was replaced with DMEM containing 10% FBS, 0.11g/L sodium pyruvate, 100U/ml penicillin and 100µg/ml

streptomycin at 37ºC/5% CO_2 for up to 5 days, with media changes every 2 days. Cells were serum starved for at least 4h, washed in warmed phosphate buffered saline (Sigma-Aldrich, St Louis, MO, USA), and plates rapidly frozen at -80°C until use. Total RNA was extracted using TriReagent® as per the manufacturer's instructions. The yield and quality of RNA was assessed by measuring absorbance at 260 and 280nm (Nanodrop ND-1000 Spectrophotometer; NanoDrop Technologies LLC, Wilmington, DE, US) and by visualisation on a 1.3% agarose gel. All RNA samples were stored at -80°C. For preparation of cDNA, 0.5µg of RNA was reverse-transcribed using iScript Reverse Transcription Supermix for qRT-PCR (Bio-Rad, Hercules, CA, USA) according to the manufacturer's instructions. Briefly, the reactions consisted of 2µL of 5 x iScript reverse transcription supermix, 3µL DNase/RNase free water, and 0.5µg of RNA, in a final volume of 10µL in 200µL Eppendorf PCR tubes. Reactions were performed on an Applied Biosystems 2720 Thermal Cycler (Applied Biosystems, Foster City, CA, USA) as follows: 25ºC for 5 min, 42ºC for 30 min, 85ºC for 5 min, and then cool to 4ºC. The cDNA was diluted with 190µL DNase/RNase free water to obtain the equivalent of 2.5ng/µL of starting RNA, and stored at -20ºC. qPCR was performed in duplicate using TaqMan Gene Expression assays (Life Technologies, Waltham, MA, USA) for B2m (Rn00560865_m1), Adra1a (Rn00567876_m1) and GPR55 (Rn03037213_s1). Each reaction consisted of 4µL cDNA, 0.5µL TaqMan Gene Expression Assay, 0.5µL DNAse/RNase free water, and 5µL TaqMan Fast Advanced Master Mix (Life Technologies, Waltham, MA, USA) dispensed in BioRad 384-well PCR plates. qRT-PCR reactions were carried out using a CFX384 Touch Realtime PCR Detection System (Bio-Rad, Hercules, CA, USA). After initial heating at 50°C for 2 min and denaturation at 95°C for 1 min, fluorescence was detected over 40 cycles (95°C for 15 sec, 60°C for 2 min). C_q values were automatically calculated by the Bio-

Rad analysis module. Data are expressed as expression of the gene of interest relative to B2m, calculated as ($2^{-\Delta Cq}$). The MIQE (Minimum Information for Publication of Quantitative Real-Time PCR Experiments) guidelines were followed [40].

2.8. Cardiomyocyte Signalling Studies

Neonatal rat ventricular cardiomyocytes were plated in 96-well plates at 50,000 cells/well grown for 5 days and serum starved overnight before experiments were performed. To investigate any crosstalk between GPR55 and α_{1A}-AR we determined the effects of GPR55 and α_{1A}-AR antagonism on downstream activation (extracellular signal-regulated kinase 1/2 (ERK1/2) phosphorylation) of the receptors. ERK1/2 phosphorylation was chosen as an indicator of receptor activation as this signalling pathway is initiated following selective activation of GPR55 by LPI, while LPI mediated changes in intracellular Ca^{2+} $[Ca^{2+}]_i$ can be induced via both GPR55 dependent and independent mechanisms [41]. In contrast, either ERK1/2 phosphorylation or changes in $[Ca^{2+}]_i$ reflect selective activation of α_{1A}-AR by A61603 [42], therefore ERK1/2 phosphorylation was chosen to enable comparison of GPR55 and α_{1A}-AR mediated signalling. Following serum starvation, cells were incubated with antagonists (CID16020046 (GPR55 antagonist; 10-100μM) or tamsulosin (α_1-AR antagonist; 10nM)) for 30min at 37°C prior to the addition of either LPI (GPR55 agonist; 10^{-10}-10^{-5}M) or A61603 (α_{1A}-AR agonist; 10^{-10}-10^{-5}M) for 5min and cells subsequently lysed. ERK1/2 (Thr202/Tyr204) phosphorylation was determined in cell lysates using an AlphaScreen SureFire assay kit (PerkinElmer; Waltham, MA, USA) as per the manufacturer's instructions. Plates were read using a multilabel plate reader (EnVision 2103; excitation wavelength 680nm and emission wavelength 520–620nm). In each

experiment three replicates were included to generate one data point and three or more independent experiments were carried out.

2.9. Statistical Analysis

For both the isolated blood vessel and ERK1/2 phosphorylation studies, nonlinear regression (three-parameter Hill equation) was used to generate concentration response curves for all data. pK_B values were calculated using the following equation: pK_B = log(conc.ratio - 1) - log(antagonist conc.). BRET saturation curves were generated using non-linear regression assuming one site binding. Concentration responses between groups were compared via a repeated measures ANOVA and Bonferroni post-hoc test. E_{max} values (maximal relaxation as a percentage of induced tone) and maximal fold changes in ERK1/2 phosphorylation were compared using either a t-test or a one-way ANOVA & Dunnett's post-hoc test as appropriate. Pressure volume loop data was subjected to multiple two-way ANOVA's and Bonferroni post-hoc tests to determine the effects of both dose and strain on adrenoceptor mediated changes in cardiac function. qRT-PCR and immunoblot data were compared using unpaired T-tests. All data was expressed as the mean±SEM and significance was determined as $P<0.05$. GraphPad Prism 8 was used to plot all curves and carry out all statistical analysis.

3. Results

3.1. Deletion of GPR55 leads to enhanced α_{1A}-AR mediated inotropic and pressor responses in mice

Baseline measurements of load-dependent indices of left ventricular systolic and diastolic function in $GPR55^{-/-}$ mice did not differ from those recorded in WT mice (Table

I), although GPR55$^{-/-}$ mice exhibited significantly elevated systolic (SBP) and mean arterial (MABP) blood pressures and heart rate (HR) compared to WT mice (P<0.05 for all; Table I). In WT mice, incremental doses (0.2-20 μg kg^{-1}) of the selective α_{1A}-AR agonist A61603 produced a dose-dependent increase in end-systolic pressure (ESP; Figure 1A) and arterial elastance (E_a; Fig 1B), with smaller concomitant rises in end-diastolic pressure (EDP; Figure 1C). These responses were abolished by prazosin and are consistent with α_{1A}-AR-mediated peripheral vasoconstriction. At 2μg kg^{-1} (but not at other doses tested) A61603 also increased dP/dt_{max} in WT mice (Figure 1D). In GPR55$^{-/-}$ mice, A61603-mediated increases in ESP, EDP and E_a were markedly exaggerated (all P<0.05) and were only partially reversed by prazosin (Figure 4A-C). Moreover, A61603 produced a significant increase in dP/dt_{max} that was not reversed by prazosin in GPR55$^{-/-}$ mice (Figure 1D). Other effects of A61603 on cardiac function (reductions in stroke volume (SV), ejection fraction (EF), and cardiac output (CO)) did not differ significantly between GPR55$^{-/-}$ and WT mice (Figure 2A-C), while HR, dP/dt_{min}, EDV, and ESV were all unaffected by α_{1A}-AR activation in both strains of mice (Figure 2D-G). To determine effects of GPR55 activation on cardiac performance, increasing doses (10, 30 & 100μg kg^{-1}) of LPI were administered to WT mice but had no significant effects on indices of either systolic or diastolic function when compared to vehicle (0.4% dimethyl sulfoxide (DMSO)) (Table II), demonstrating that direct activation of GPR55 *per se* does not induce a functional haemodynamic response.

3.2. α_{1A}-AR expression is downregulated in the hearts of GPR55$^{-/-}$ mice

Analysis of ventricular tissue demonstrated that both gene (mRNA) and protein expression of α_{1A}-AR were significantly lower in GPR55$^{-/-}$ mice compared to WT mice (both P<0.05; Figure 3A & B), which suggests that a greater abundance of the receptor

is not responsible for the enhanced functional response but does not rule out the possibility of increased sensitivity of α_{1A}-ARs to A61603 in mice lacking GPR55.

3.3. GPR55 deletion enhances, while GPR55 antagonism suppresses, α_{1A}-AR mediated vasoconstriction

Since the *in vivo* studies above revealed an exaggerated increase in afterload in response to A61603 in GPR55$^{-/-}$ mice, we examined contractile responses to α_{1A}-AR stimulation in isolated blood vessels. In carotid arteries isolated from WT mice, A61603 produced a concentration-dependent contractile response that was antagonised by the α_{1A}-AR antagonist tamsulosin (P<0.001; Figure 4A). Tamsulosin antagonised A61603 induced vasoconstriction with an estimated pK_B value of 10.26 which is consistent with previously reported antagonism at α_{1A}-ARs [43,44]. In contrast, contractile responses to A61603 were significantly augmented in vessels isolated from GPR55$^{-/-}$ mice (E_{max}: 4.26±0.59 vs. 2.81±0.55mN/mm; P<0.05; Figure 4B). At the highest concentration (100μM) tested, the selective GPR55 antagonist CID16020046 induced a rightward shift in the A61603 mediated contractile response in arteries from WT (P<0.05; Figure 4C), but not GPR55$^{-/-}$ mice (Figure 4D). To examine whether tamsulosin or CID16020046 altered the effects of a known GPR55 agonist, a concentration response was carried out with LPI, which produced a modest (E_{max}: 23.9±4.67%) vasorelaxant response (determined in arteries pre-contracted with U46619) in WT vessels (Figure 5A). LPI failed to produce a response in vessels from GPR55$^{-/-}$ mice (Figure 5A) or in the presence of the GPR55 antagonist CID16020046 (Figure 5B), but its vasodilator action persisted in the presence of tamsulosin (10nM; Figure 5C), confirming its action at GPR55.

3.4. GPR55 and α_{1A}-AR do not dimerise, but crosstalk exists between the two receptors

The heightened responses to α_{1A}-AR activation in the absence of GPR55 strongly suggests that the two receptors interact at some level. While the receptors co-localise in some vascular cells [5], it is not known whether they dimerise or modulate each other's downstream signalling. We therefore performed BRET analysis in CHO-K1 cells to determine whether receptor dimers form between α_{1A}-AR and GPR55. While the saturation curve for α_{1A}-AR and V2R receptor clearly demonstrated dimerization [36] and was used as a positive control (Figure 6A), no dimerization of the α_{1A}-AR with GPR55 was evident (Figure 6B). In separate studies, A61603 and LPI induced ERK1/2 phosphorylation in CHO-K1 cells transiently transfected with tagged (i.e. Rluc8 or Venus) constructs encoding α_{1A}-AR and GPR55, respectively, confirming that the addition of the tag did not alter the activity of the construct (Figure 7A & B). To determine signalling interaction, we examined whether α_{1A}-AR-mediated increases in ERK1/2 phosphorylation in neonatal rat ventricular cardiomyocytes was influenced by GPR55. qPCR experiments carried out confirmed the expression of both α_{1A}-AR and GPR55 in neonatal rat ventricular cardiomyocytes, which is in agreement with previous studies carried out by Sato et al. (α_{1A}-AR) [28] and Yu et al. (GPR55) [8] (Figure 8). Furthermore, the expression of α_{1A}-AR appeared to be approximately 2-fold higher than that of GPR55 in neonatal rat ventricular cardiomyocytes (Figure 8). A61603 produced a concentration-dependent increase (6-fold increase at 10μM; Figure 9A & Table III) in ERK1/2 phosphorylation, that was attenuated by both α_{1A}-AR (tamsulosin; Figure 9A & Table III) and GPR55 (CID16020046; Figure 9B & Table III) blockade. In contrast, while LPI induced a transient and modest increase in ERK1/2 phosphorylation (~2-fold at 10μM: Figure 9C & Table III), this was only reduced by

CID16020046, but not tamsulosin (Figure 9C & D & Table III). Thus, GPR55 appears to regulate α_{1A}-AR signalling, whereas the reverse does not appear to hold true.

4. Discussion

4.1. α_{1A}-AR-activation increases cardiac function in WT mice

Previous studies demonstrate a direct inotropic effect following α_{1A}-AR activation, largely based on studies in rats, either *in vivo* [14,18] or in isolated cardiac tissue preparations [16]. Rat heart shows high expression of myocardial α_{1A}-ARs; much higher (~5-fold) than in either human or mouse hearts [45] and in mouse hearts α_{1A}-ARs are present in ~50% (highly expressed in 20%) of cardiomyocytes [46]. However, in human myocardial tissue, inotropic responses to α_1-AR activation have been reported as early as 1980 [47], with more recent work indicating that even relatively low α_{1A}-AR densities can elicit an inotropic response [17]. In mice, the inotropic response to α_{1A}-AR activation has been little studied, although transgenic mice over-expressing α_{1A}-ARs exhibit a marked increase in baseline cardiac contractility that is resistant to β_1-AR blockade [48]. Moreover, α_{1A}-AR stimulation of cultured cardiomyocytes elicits either a heterogeneous inotropic response to phenylephrine [49], or an exaggerated response to the selective α_{1A}-AR agonist A61603, associated with increased release of $[Ca^{2+}]_i$ [50]. Here we show that *in vivo* administration of A61603 to WT mice causes a prazosin-sensitive increase in cardiac function (ESP and dP/dt_{max}), demonstrating an α_{1A}-AR-mediated positive inotropic response. This is consistent with previous *in vivo* studies in pithed rats (no baroreceptor reflex to correct for changes in peripheral resistance) demonstrating a positive inotropic response to phenylephrine. Here, the animals had an intact central nervous system, showing that

even in the presence of functioning baroreceptor reflexes a positive inotropic response to α_{1A}-AR activation is still present.

4.2. Interactions between GPR55 and α_{1A}-ARs on cardiac function

We showed that GPR55 deletion has no impact on baseline cardiac contractile function (dP/dt_{max}, ESPVR or E_{max}), while intravenous administration of LPI in WT mice did not alter indices of cardiac contractile function, confirming previous findings [6]. Although LPI induces a GPR55-mediated increase in $[Ca^{2+}]_i$ in cultured cardiomyocytes [8], our data shows that this does not translate into a functional inotropic response. While it's plausible that activation of GPR55 *in vivo* does not directly affect contractile activity (supported by the lack of effect of GPR55 gene deletion on several Ca^{2+} dependent indices of contractility (dP/dt_{max}, ESPVR or E_{max})), it should also be considered that the concentration range (10-100μg kg^{-1}) of LPI used in the present study may not have been sufficient to elicit a measurable response, as it appears micromolar concentrations are required to elicit both physiological [8] and pathophysiological [51] responses in cardiomyocytes/hearts. In contrast, inotropic responses to A61603 were markedly exaggerated in GPR55$^{-/-}$ mice, suggesting that rather than the GPR55/LPI system directly influencing cardiac contractile activity, GPR55 acts as a sentinel receptor that negatively regulates α_{1A}-AR function. To determine whether enhanced responses to α_{1A}-AR activation in the absence of GPR55 resulted from increased cardiac expression of α_{1A}-ARs we examined expression in the myocardium and found, surprisingly, that both α_{1A}-AR mRNA and protein were reduced in the hearts of GPR55$^{-/-}$ mice. While this suggested crosstalk between these two receptors, it was somewhat counter-intuitive to the functional data but could nevertheless represent a compensatory response to the loss of negative control of α_{1A}-ARs imposed by GPR55.

While both the inotropic response and changes in E_a induced by A61603 were blocked by prazosin in WT mice, this was not the case in GPR55$^{-/-}$ mice where a significant residual response remained. The likelihood of an "off-target" effect of A61603 is low since it is highly selective for α_{1A}-ARs (pEC_{50} 7.8-8.4) [52]. However, it does question the location of, and drug accessibility to, α_{1A}-AR and GPR55 receptors. There is growing evidence that α_{1A}-ARs localised in the nuclear membrane are responsible for the positive inotropic response to α_{1A}-AR agonists (reviewed in [53]). Although prazosin is reported to be membrane permeable and blocks the actions of phenylephrine at nuclear α_{1A}-ARs in isolated cardiomyocytes [54], it has yet to be established whether this occurs *in vivo*. Cardiomyocyte GPR55 receptors are localised both to the sarcolemmal membrane and on endolysosomal membranes [8]. Crosstalk could therefore occur between the intracellular, rather than sarcolemmal, α_{1A}-AR and GPR55 receptors.

4.3. Crosstalk between GPR55 and α_{1A}-ARs in the vasculature

GPR55$^{-/-}$ mice exhibited increased arterial blood pressure, consistent with a role for GPR55 in the control of vascular tone. GPR55 activation by LPI induces endothelial cell hyperpolarization [55], relaxes isolated mesenteric arteries [7], and decreases DBP in pithed rats [22]. Moreover, the serum concentration range of LPI (2-4μM) in rodents [56,57] is similar to the concentrations required to relax resistance vessels, suggesting that GPR55 activation by circulating LPI contributes to suppression of vascular tone in mice and the corollary of this would be elevated blood pressure in the absence of GPR55.

In isolated blood vessels, the vasoconstrictor response to A61603 was enhanced in GPR55$^{-/-}$ mice. Thus, as in the heart, GPR55 appears to influence α_{1A}-AR-mediated responses in the vascular tissue, supported by observations that LPI attenuates α_1-AR mediated elevations in DBP [22] by a CBD sensitive receptor (most likely GPR55). Previous unpublished work from this group has demonstrated that unlike A61603, U46619 (thromboxane A2 receptor agonist) and 5-hydroxytryptamine (5-hydroxytryptamine 2A receptor agonist) induced contractile responses do not differ in arteries from WT and GPR55$^{-/-}$ mice. While this may suggest that genetic deletion of GPR55 primarily effects α_{1A}-AR-mediated vasoconstriction, an effect on other contractile receptors (i.e. endothelin receptor A, angiotensin II type-1 receptor etc.) cannot be ruled out. In vessels from WT mice, the GPR55 antagonist (CID16020046) at high concentrations depressed responses to A61603. An “off target” effect of CID16020046 is unlikely since it did not influence A61603 responses in blood vessels from GPR55$^{-/-}$ mice, confirming its specificity at GPR55. This raises the intriguing question as to whether loss of receptor protein and receptor blockade have different impacts on α_{1A}-AR function. In carotid arteries, LPI induced a small (compared to that previously reported in resistance vessels i.e. ~70% [7]), but measurable (~20%) vasodilator response, previously associated with an endothelial site of action [7]. This was unaffected by α_{1A}-AR blockade with tamsulosin, but was inhibited by CID16020046, which may be explained by reports of co-expression of both GPR55 and α_{1A}-ARs on vascular smooth muscle cells (VSMCs), but only GPR55 on the endothelium [5]. In this setting, CID16020046 acting on VSMC expressed GPR55 could influence α_{1A}-AR induced vasoconstriction, however as α_{1A}-ARs are not expressed on endothelial cells tamsulosin would be ineffectual against GPR55 induced vasodilation, which has previously been shown to be endothelial dependent [7]. Finally,

this data suggests that, while GPR55 controls α_{1A}-AR responses, the reverse does not apply.

4.4. GPR55 influences signalling of α_{1A}-ARs in cardiomyocytes, but not by receptor heterodimerisation

Since both GPR55 and α_{1A}-ARs form heteromers with other receptors [11-13,58,59,], and co-localise in some vascular cells [5], we determined whether the functional interaction between these receptors could be explained by heteromerization between GPR55 and α_{1A}-ARs. However, BRET analysis in CHO-K1 cells demonstrated that while vasopressin 2 receptor (V2R) and α_{1A}-ARs dimerize (indicating their close proximity), GPR55 and α_{1A}-ARs do not form dimers, suggesting that the functional interactions between the two receptors are likely due to regulation of α_{1A}-AR signalling by GPR55. Indeed, in neonatal cardiomyocytes, we showed that blockade of GPR55 with CID16020046 prevents α_{1A}-AR-mediated ERK1/2 phosphorylation in response to A61603. Conversely, tamsulosin did not affect LPI induced ERK1/2 phosphorylation in cardiomyocytes and the reason for this is unclear as both receptors are expressed in these cells.

4.5. Conclusions

Our findings demonstrate that although GPR55 and α_{1A}-AR do not dimerize, GPR55 regulates both the signalling and functional activity of α_{1A}-AR, while the latter does not appear to influence the activity of GPR55. At present it is unclear why genetic deletion of GPR55 enhances α_{1A}-AR function whereas pharmacological blockade of GPR55 appears to impede activity, though it is possible that a functional adaption occurs in our global knockout mouse model that is lacking in the ‘conditional knockout’ model

reflected by pharmacological blockade of GPR55 in both cardiomyocytes and isolated arteries. Notwithstanding this, we demonstrate a novel role for GPR55 in the regulation of α_{1A}-AR activity, that may represent a novel target for the development of treatments for conditions characterised by aberrant activity of both GPR55 and α_{1A}-AR such as prostate cancer, hypertension or heart failure.

Abbreviations: α_{1A}-AR, α_{1A}-adrenoceptor; β_1-AR, β_1-adrenoceptor; β_2-AR, β_2-adrenoceptor; $[Ca^{2+}]_i$, intracellular calcium; CB_1, cannabinoid 1 receptor; CB_2, cannabinoid 2 receptor; CBD, cannabidiol; CO, cardiac output; DBP, diastolic blood pressure; DOCA, Deoxycorticosterone acetate; E_a arterial elastance; EDP, end diastolic pressure; EDV, end diastolic volume; EF, ejection fraction; ESP, end systolic pressure; ESV, end systolic volume; ESPVR, end systolic pressure volume relationship; $GPR55^{-/-}$, GPR55 knockout; HR, heart rate; IP_3, inositol triphosphate; LPI, lysophosphatidylinositol; LTCC, l-type Ca^{2+} channel; MABP, mean arterial blood pressure; SBP, systolic blood pressure; SV, stroke volume; SW, stroke work; V2R, Vasopressin 2 receptor; WT, wild-type.

Acknowledgements

The original heterozygous GPR55 knockout mice breeding pairs were kindly provided by AstraZeneca (Gothenburg, Sweden). This work was supported by an Integrative Pharmacology Fund Pump Priming Grant from the British Pharmacological Society and a Research Incentive Grant (grant 70754) from The Carnegie Trust for the Universities of Scotland (both awarded to Sarah K Walsh). This work was also supported by the National Health and Medical Research Council of Australia (grant 1129667 awarded

to Masaaki Sato and Dana S Hutchinson). The graphical abstract was created with BioRender.com

Author Contributions

Conceptualization: Sarah K Walsh, Sheng Y Ang, Martina Kocan, Dana S Hutchinson, Roger J Summers & Cherry L Wainwright. Investigation: Sarah K Walsh, Christopher Lipina, Sheng Y Ang, Ling Yeong Chia, Masaaki Sato & Dana S Hutchinson. Formal analysis: Sarah K Walsh, Christopher Lipina, Masaaki Sato & Dana S Hutchinson. Writing – Original draft: Sarah K Walsh, Christopher Lipina, Sheng Y Ang & Dana S Hutchinson. Writing – Review & Editing: Martina Kocan, Roger J Summers & Cherry L Wainwright. Funding acquisition: Sarah K Walsh, Masaaki Sato & Dana S Hutchinson.

Conflict of interest

The authors declare no conflicts of interest.

References

1. Sawzdargo M, Nguyen T, Lee DK, Lynch KR, Cheng R, Heng HH, George SR, O'Dowd BF (1999). Identification and cloning of three novel human G protein-coupled receptor genes GPR52, ψGPR53 and GPR55: GPR55 is extensively expressed in human brain. *Brain Res Mol Brain Res* 64: 193-198. DOI: 10.1016/s0169-328x(98)00277-0.
2. Oka S, Nakajima K, Yamashita A, Kishimoto S, Sugiura T (2007). Identification of GPR55 as a lysophosphatidylinositol receptor. *Biochem Biophys Res Commun* 362: 928-34. DOI: 10.1016/j.bbrc.2007.08.078.

3. Henstridge CM, Balenga NA, Kargl J, Andradas C, Brown AJ, Irving A, Sanchez C, Waldhoer M (2011). Minireview: recent developments in the physiology and pathology of the lysophosphatidylinositol-sensitive receptor GPR55. *Mol Endocrinol* 25: 1835-1848. DOI: 10.1210/me.2011-1197.
4. Ryberg E, Larsson N, Sjögren S, Hjorth S, Hermansson NO, Leonova J, Elebring T, Nilsson K, Drmota T, Greasley PJ (2007). The orphan receptor GPR55 is a novel cannabinoid receptor. *Br J Pharmacol* 152: 1092-1101. DOI: 10.1038/sj.bjp.0707460.
5. Daly CJ, Ross RA, Whyte J, Henstridge CM, Irving AJ, McGrath JC (2010). Fluorescent ligand binding reveals heterogenous distribution of adrenoceptors and 'cannabinoid-like' receptors in small arteries. *Br J Pharmacol* 159: 787-796. DOI: 10.1111/j.1476-5381.2009.00608.x.
6. Walsh SK, Hector EE, Andréasson AC, Jönsson-Rylander AC, Wainwright CL (2014). GPR55 deletion in mice leads to age-related ventricular dysfunction and impaired adrenoceptor-mediated inotropic responses. *PLoS One* 9: e108999. DOI: 10.1371/journal.pone.0108999.
7. AlSuleimani YM, Hiley CR (2015). The GPR55 agonist lysophosphatidylinositol relaxes rat mesenteric resistance artery and induces Ca(2+) release in mesenteric artery endothelial cells. *Br J Pharmacol* 172: 3043-3057. DOI: 10.1111/bph.13107.
8. Yu J, Deliu E, Zhang XQ, Hoffman NE, Carter RL, Grisanti LA, Brailoiu GC, Madesh M, Cheung JY, Force T, Abood ME, Koch WJ, Tilley DG, Brailoiu E (2013). Differential activation of cultured neonatal cardiomyocytes by plasmalemmal vs intracellular G protein-coupled receptor 55. *J Biol Chem* 288: 22481-22492. DOI: 10.1074/jbc.M113.456178.

9. Ali RM, Al Kury LT, Yang KH, Qureshi A, Rajesh M, Galadari S, Shuba YM, Howarth FC, Oz M (2015). Effects of cannabidiol on contractions and calcium signalling in rat ventricular myocytes. *Cell Calcium* 57: 290-299. DOI: 10.1016/j.ceca.2015.02.001.

10. Kargl J, Balenga N, Parzmair GP, Brown AJ, Heinemann A, Waldhoer M (2010). The cannabinoid receptor CB1 modulates the signalling properties of the lysophosphatidylinositol receptor GPR55. *J Biol Chem* 287: 44234-44248. DOI: 10.1074/jbc.M112.364109.

11. Martínez-Pinilla E, Rico AJ, Rivas-Santisteban R, Lillo J, Roda E, Navarro G, Franco R, Lanciego JL (2020). Expression of cannabinoid CB_1R-GPR55 heteromers in neuronal subtypes of the Macaca fascicularis striatum. *Ann N Y Acad Sci* DOI: 10.1111/nyas.14413.

12. Balenga NA, Martínez-Pinilla E, Kargl J, Schröder R, Peinhaupt M, Platzer W, Bálint Z, Zamarbide M, Dopeso-Reyes IG, Ricobaraza A, Pérez-Ortiz JM, Kostenis E, Waldhoer M, Heinemann A, Franco R (2014). Heteromerization of GPR55 and cannabinoid CB2 receptors modulates signalling. *Br J Pharmacol* 171: 5387-5406. DOI: 10.1111/bph.12850.

13. Moreno E, Andradas C, Medrano M, Caffarel MM, Pérez-Gómez E, Blasco-Benito S, Gómez-Cañas M, Pazos MR, Irving AJ, Lluís C, Canela EI, Fernández-Ruiz J, Guzmán M, McCormick PJ, Sánchez C (2014). Targeting CB2-GPR55 receptor heteromers modulates cancer cell signalling. *J Biol Chem* 289: 21960-21972. DOI: 10.1074/jbc.M114.561761.

14. Ruffolo RR Jr, Messick K (1985). Inotropic selectivity of dobutamine enantiomers in the pithed rat. *J Pharmacol Exp Ther* 235: 344-348.

15. Skomedal T, Schiander IG, Osnes JB (1988). Both alpha and beta adrenoceptor-mediated components contribute to final inotropic response to norepinephrine in rat heart. *J Pharmacol Exp Ther* 247: 1204-1210.

16. Nagashima M, Hattori Y, Tohse N, Kanno M (1997). Alpha 1-adrenoceptor subtype involved in the positive and negative inotropic responses to phenylephrine in rat papillary muscle. *Gen Pharmacol* 28: 721-725. DOI: 10.1016/s0306-3623(96)00356-4.

17. Janssen PML, Canan BD, Kilic A, Whitson BA, Baker AJ (2018). Human myocardium has a robust α1A-subtype adrenergic receptor inotropic response. *J Cardiovasc Pharmacol* 72: 136-142. DOI: 10.1097/FJC.0000000000000604.

18. Broadley KJ, Williamson KL, Roach AG (1999). In vivo demonstration of alpha-adrenoceptor-mediated positive inotropy in pithed rats: evidence that noradrenaline does not stimulate myocardial alpha-adrenoceptors. *J Auton Pharmacol* 19: 55-63. DOI: 10.1046/j.1365-2680.1999.00115.x.

19. Bach HH, Wong YM, Tripathi A, Nevins AM, Gamelli RL, Volkman BF, Byron KL, Majetschak M (2014). Chemokine (C-X-C motif) receptor 4 and atypical chemokine receptor 3 regulate vascular α_1-adrenergic receptor function. *Mol Med* 20: 435-47. DOI: 10.2119/molmed.2014.00101.

20. Albee LJ, Eby JM, Tripathi A, LaPorte HM, Gao X, Volkman BF, Gaponenko V, Majetschak M (2017). α1-Adrenergic receptors function within hetero-oligomeric complexes with atypical Chemokine Receptor 3 and Chemokine (C-X-C motif) Receptor 4 in vascular smooth muscle cells. *J Am Heart Assoc* 6 e006575. DOI: 10.1161/JAHA.117.006575.

21. Bender SB, Klabunde RE (2007). Altered role of smooth muscle endothelin receptors in coronary endothelin-1 and alpha1-adrenoceptor-mediated

vasoconstriction in Type 2 diabetes. *Am J Physiol Heart Circ Physiol* 293: H2281-2288. DOI: 10.1152/ajpheart.00566.2007.

22. Marichal-Cancino BA, Manrique-Maldonado G, Altamirano-Espinoza AH, Ruiz-Salinas I, González-Hernández A, Maassenvandenbrink A, Villalón CM (2013). Analysis of anandamide- and lysophosphatidylinositol-induced inhibition of the vasopressor responses produced by sympathetic stimulation or noradrenaline in pithed rats. *Eur J Pharmacol* 721: 168-177. DOI: 10.1016/j.ejphar.2013.09.039.
23. Patil KC, McPherson L, Daly CJ (2015). Co-localization of alpha1-adrenoceptors and GPR55: a novel prostate cancer paradigm? *Pharmacol Pharm* 6: 212-220.
24. Kneale BJ, Chowienczyk PJ, Brett SE, Coltart DJ, Ritter JM (2000). Gender differences in sensitivity to adrenergic agonists of forearm resistance vasculature. *J Am Coll Cardiol* 36: 1233-1238. DOI: 10.1016/s0735-1097(00)00849-4.
25. McKee AP, Van Riper DA, Davison CA, Singer HA (2003). Gender-dependent modulation of alpha 1-adrenergic responses in rat mesenteric arteries. *Am J Physiol Heart Circ Physiol* 284: 1737-1743. DOI: 10.1152/ajpheart.00779.2002.
26. Percie du Sert N, Hurst V, Ahluwalia A, Alam S, Avey MT, Baker M, Browne WJ, Clarke A, Cuthill IC, Dirnagl U, Emerson M, Garner P, Holgate ST, Howells DW, Karp NA, Lazic SE, Lidster K, MacCallum CJ, Macleod M, Pearl EJ, Petersen OH, Rawle F, Reynolds P, Rooney K, Sena ES, Silberberg SD, Steckler T, Wurbel H (2020). The ARRIVE guidelines 2.0: updated guidelines for reporting animal research. *PLoS Biol* 18: e3000410. DOI: 10.1113/JP280389.

27. Pacher P, Nagayama T, Mukhopadhyay P, Bátkai S, Kass DA (2008). Measurement of cardiac function using pressure-volume conductance catheter technique in mice and rats. *Nat Protoc* 3: 1422-1434. DOI: 10.1038/nprot.2008.138.

28. Sato M, Evans BA, Sandström AL, Chia LY, Mukaida S, Thai BS, Nguyen A, Lim L, Tan CYR, Baltos JA, White PJ, May LT, Hutchinson DS, Summers RJ, Bengtsson T (2018). α_{1A}-Adrenoceptors activate mTOR signalling and glucose uptake in cardiomyocytes. *Biochem Pharmacol* 148: 27-40. DOI: 10.1016/j.bcp.2017.11.016.

29. Mathar I, Vennekens R, Meissner M, Kees F, van der Mieren G, Camacho Londono JE, Uhl S, Voets T, Hummel B, van den Bergh A, Herijgers P, Nilius B, Flockerzi V, Schweda F, Freichel M (2010). Increased catecholamine secretion contributes to hypertension in TRPM4-deficient mice. *J Clin Invest* 120: 3267-3279. DOI: 10.1172/JCI41348.

30. Musakawa D, Koga M, Sezaki A, Nakao Y, Kamikubo Y, Hashimoto T, Okuyama-Oki Y, Aladeokin AC, Nakamura F, Yokoyama U, Wakui H, Ichinose H, Sakurai T, Umemura S, Tamura K, Ishikawa Y, Goshima Y (2017). L-DOPA sensitizes vasomotor tone by modulating the vascular alpha1-adrenergic receptor. *JCI Insight* 2: e90903. DOI: 10.1172/jci.insight.90903.

31. MacGowan GA, Rager J, Shroff SG, Mathier MA (2005). In vivo alpha-adrenergic responses and troponin I phosphorylation: anesthesia interactions. *J Appl Physiol* 98: 1163-1170. DOI: 10.1152/japplphysiol.00959.2004.

32. Methven L, Simpson PC, McGrath JC (2009). Alpha1A/B-knockout mice explain the native alpha1D-adrenoceptor's role in vasoconstriction and show that its

location is independent of the other alpha1-subtypes. *Br J Pharmacol* 158: 1663-1675. DOI: 10.1111/j.1476-5381.2009.00462.x.

33. Kargl J, Brown AJ, Andersen L, Dorn G, Schicho R, Waldhoer M, Heinemann A (2013). A selective antagonist reveals a potential role of G protein-coupled receptor 55 in platelet and endothelial cell function. *J Pharmacol Exp Ther* 346: 54-66. DOI: 10.1124/jpet.113.204180.
34. Pfaffl MW (2001). A new mathematical model for relative quantification in real-time RT-PCR. *Nucleic Acids Res* 29: e45. DOI: 10.1093/nar/29.9.e45.
35. Hajduch E, Alessi DR, Hemmings BA, Hundal HS (1998). Constitutive activation of protein kinase B alpha by membrane targeting promotes glucose and system A amino acid transport, protein synthesis, and inactivation of glycogen synthase kinase 3 in L6 muscle cells. *Diabetes* 47: 1006-1013. DOI: 10.2337/diabetes.47.7.1006.
36. Mustafa S, See HB, Seeber RM, Armstrong SP, White CW, Ventura S, Ayoub MA, Pfleger KDG (2012). Identification and profiling of novel α1A-adrenoceptor-CXC chemokine receptor 2 heteromer. *J Biol Chem* 287: 12952-12965. DOI: 10.1074/jbc.M111.322834.
37. Evans BA, Broxton N, Merlin J, Sato M, Hutchinson DS, Christopoulos A, Summers RJ (2010). Quantification of functional selectivity at the human α_{1A}-adrenoceptor. *Mol Pharmacol* 79: 298-307. DOI: 10.1124/mol.110.067454
38. Kocan M, See HB, Seeber RM, Eidne KA, Pfleger KD (2008). Demonstration of improvements to the bioluminescence resonance energy transfer (BRET) technology for the monitoring of G protein-coupled receptors in live cells. J *Biomol Screen* 13: 888–898. DOI: 10.1177/1087057108324032.

39. Kocan M, See HB, Sampaio NG, Eidne KA, Feldman BJ, Pfleger KD (2009). Agonist-independent interactions between beta-arrestins and mutant vasopressin type II receptors associated with nephrogenic syndrome of inappropriate antidiuresis. *Mol Endocrinol* 23: 559–571. DOI: 10.1210/me.2008-0321.

40. Bustin SA, Benes V, Garson JA, Hellemans J, Huggett J, Kubista M, Mueller R, Nolan T, Pfaffl MW, Shipley GL, Vandesompele J, Wittwer CT (2009). The MIQE Guidelines: Minimum information for the publication of quantitative real-time PCR experiments. *Clin Chem* 55: 611-622. DOI: 10.1373/clinchem.2008.112797.

41. Oka S, Toshida T, Maruyama K, Nakajima K, Yamashita A, Sugiura T (2009). 2-Arachidonoyl-sn-glycero-3-phosphoinositol: a possible natural ligand for GPR55. *J Biochem* 145: 13-20. DOI: 10.1093/jb/mvn136.

42. da Silva Junior ED, Sato M, Merlin J, Broxton N, Hutchinson DS, Ventura S, Evans BA, Summers RJ (2017). Factors influencing biased agonism in recombinant cells expressing the human α_{1A} -adrenoceptor. *Br J Pharmacol* 174: 2318-2333. DOI: 10.1111/bph.13837.

43. Lachnit WG, Tran AM, Clarke DE, Ford AP (1997). Pharmacological characterization of an alpha $_{1A}$-adrenoceptor mediating contractile responses to noradrenaline in isolated caudal artery of rat. *Br J Pharmacol* 120: 819-826. DOI: 10.1038/sj.bjp.0700983.

44. Chang DJ, Chang TK, Yamanishi SS, Salazar FH, Kosaka AH, Khare R, Bhakta S, Jasper JR, Shieh IS, Lesnick JD, Ford AP, Daniels DV, Eglen RM, Clarke DE, Bach C, Chan HW (1998). Molecular cloning, genomic characterization and

expression of novel human alpha$_{1A}$-adrenoceptor isoforms. *FEBS Lett* 422: 279-283. DOI: 10.1016/s0014-5793(98)00024-6.

45. Steinfath M, Chen YY, Lavický J, Magnussen O, Nose M, Rosswag S, Schmitz W, Scholz H (1992). Cardiac alpha 1-adrenoceptor densities in different mammalian species. *Br J Pharmacol* 107: 185-188. DOI: 10.1111/j.1476-5381.1992.tb14484.x

46. Myagmar BE, Flynn JM, Cowley PM, Swigart PM, Montgomery MD, Thai K, Nair D, Gupta R, Deng DX, Hosoda C, Melov S, Baker AJ, Simpson PC (2017). Adrenergic receptors in individual ventricular myocytes: the Beta-1 and Alpha-1B are in all cells, the Alpha-1A is in a subpopulation, and the Beta-2 and Beta-3 are mostly absent. *Circ Res* 120: 1103-1115. DOI: 10.1161/CIRCRESAHA.117.311146.

47. Wagner J, Schumann HJ, Knorr A, Rohm N, Reidemeister JC (1980). Stimulation of adrenaline and dopamine but not by noradrenaline of myocardial alpha-adrenoceptors mediating positive inotropic effects in human atrial preparations. *Naunyn Schmiedebergs Arch Pharmacol* 312: 99-102. DOI: 10.1007/BF00502581.

48. Lin F, Owens WA, Chen S, Stevens ME, Kesteven S, Arthur JF, Woodcock EA, Feneley MP, Graham RM (2001). Targeted alpha(1A)-adrenergic receptor overexpression induces enhanced cardiac contractility but not hypertrophy. *Circ Res* 89: 343-350. DOI: 10.1161/hh1601.095912.

49. Chu C, Thai K, Park KW, Wang P, Makwana O, Lovett DH, Simpson PC, Baker AJ (2013). Intraventricular and interventricular cellular heterogeneity of inotropic responses to α(1)-adrenergic stimulation. *Am J Physiol Heart Circ Physiol* 304: H946-953. DOI: 10.1152/ajpheart.00822.2012.

50. Yu ZY, Tan JC, McMahon AC, Iismaa SE, Xiao XH, Kesteven SH, Reichelt ME, Mohl MC, Smith NJ, Fatkin D, Allen D, Head SI, Graham RM, Feneley MP (2014). RhoA/ROCK signaling and pleiotropic α1A-adrenergic receptor regulation of cardiac contractility. *PLoS One* 9: e99024. DOI: 10.1371/journal.pone.0099024.

51. Robertson-Gray OJ, Walsh SK, Ryberg E, Jönsson-Rylander AC, Lipina C, Wainwright CL (2019). l-α-Lysophosphatidylinositol (LPI) aggravates myocardial ischemia/reperfusion injury via a GPR55/ROCK-dependent pathway. *Pharmacol Res Perspect* 7: e00487. DOI: 10.1002/prp2.487.

52. Knepper SM, Buckner SA, Brune ME, DeBernardis JF, Meyer MD, Hancock AA. (1995). A-61603, a potent alpha 1-adrenergic receptor agonist, selective for the alpha 1A receptor subtype. *J Pharmacol Exp Ther* 274: 97-103.

53. Wu SC, O'Connell TD (2015). Nuclear compartmentalization of α1-adrenergic receptor signaling in adult cardiac myocytes. *J Cardiovasc Pharmacol* 65: 91-100. DOI: 10.1097/FJC.0000000000000165.

54. Wright CD, Chen Q, Baye NL, Huang Y, Healy CL, Kasinathan S, O'Connell TD (2008). Nuclear alpha1-adrenergic receptors signal activated ERK localization to caveolae in adult cardiac myocytes. *Circ Res* 103: 992-1000. DOI: 10.1161/CIRCRESAHA.108.176024.

55. Bondarenko A, Waldeck-Weiermair M, Naghdi S, Poteser M, Malli R, Graier WF (2010). GPR55-dependent and -independent ion signalling in response to lysophosphatidylinositol in endothelial cells. *Br J Pharmacol* 161: 308-320. DOI: 10.1111/j.1476-5381.2010.00744.x.

56. Bollinger JG, Li H, Sadilek M, Gelb MH (2010). Improved method for the quantification of lysophospholipids including enol ether species by liquid

chromatography-tandem mass spectrometry. *J Lipid Res* 51: 440-447. DOI: 10.1194/jlr.D000885.

57. Imbernon M, Whyte L, Diaz-Arteaga A, Russell WR, Moreno NR, Vazquez MJ, Gonzalez CR, Díaz-Ruiz A, Lopez M, Malagón MM, Ross RA, Diequez C, Noqueiras R (2014). Regulation of GPR55 in rat white adipose tissue and serum LPI by nutritional status, gestation, gender and pituitary factors. *Mol Cell Endocrinol* 383: 159-169. DOI: 10.1016/j.mce.2013.12.011.

58. Uberti MA, Hall RA, Minneman KP (2003). Subtype-specific dimerization of alpha 1-adrenoceptors: effects on receptor expression and pharmacological properties*. Mol Pharmacol* 64: 1379-1390. DOI: 10.1124/mol.64.6.1379.

59. Tripathi A, Vana PG, Chavan TS, Brueggemann LI, Byron KL, Tarasova NI, Volkman BF, Gaponenko V, Majetschak M (2015). Heteromerization of chemokine (C-X-C motif) receptor 4 with α1A/B-adrenergic receptors controls α1-adrenergic receptor function. *Proc Natl Acad Sci U S A* 112: E1659-68. DOI: 10.1073/pnas.1417564112.

Figures Legends

Figure 1. GPR55$^{-/-}$ mice exhibit an enhanced cardiovascular response to α_{1A}-AR activation. The Δ from baseline cardiac function induced by increasing doses of A61603 (0.2-20μg kg^{-1}) was calculated and data from the following functional indices; ESP (A), E_a (B), EDP (C) and dP/dt_{max} (D) presented above. To demonstrate selectivity at the α_1-AR, the highest dose of A61603 (20μg kg^{-1}) was also administered following pretreatment with prazosin (1mg kg^{-1}). Data was expressed as mean±s.e.m. *P<0.05

vs. 0μg kg^{-1} (within group); #*P*<0.05 vs. WT (equivalent dose); †*P*<0.05 vs. WT (20μg kg^{-1}); ‡*P*<0.05 vs. GPR55$^{-/-}$ (20μg kg^{-1}). n=9.

Figure 2. α_{1A}-AR mediated effects on cardiac function that were not markedly influenced by the presence or absence of GPR55. The Δ from baseline cardiac function induced by increasing doses of A61603 (0.2-20μg kg^{-1}) was calculated and data expressed as mean±SEM. To demonstrate selectivity at the α_1-AR, the highest dose of A61603 (20μg kg^{-1}) was also administered following pretreatment with prazosin (1mg kg^{-1}). **P*<0.05 vs. 0μg kg^{-1} (within group); †*P*<0.05 vs. WT (20μg kg^{-1}). n=9.

Figure 3. Mice with a genetic deletion for GPR55 are characterised by reduced cardiac expression of α_{1A}-AR. α_{1A}-AR mRNA (A) and α_{1A}-AR protein (B) expression in cardiac tissue from both WT and GPR55$^{-/-}$ mice. Quantified values are presented as the mean±SEM. **P*<0.05 vs. WT. n=4-5.

Figure 4. Effects of GPR55 and α_1-AR antagonists on A61603 induced contractile responses in isolated mesenteric arteries from WT and GPR55$^{-/-}$ mice. In (A), concentration response curves with the α_{1A}-AR agonist, A61603, carried out in mesenteric arteries from WT mice in the absence and presence of the α_1-AR antagonist, tamsulosin; in (B), comparison of A61603-induced contractile responses in vessels from both WT and GPR55$^{-/-}$ mice (B). A61603 induced vasoconstriction in the absence and presence of the GPR55 antagonist, CID16020046 (CID), and shown in isolated vessels from both WT (C) and GPR55$^{-/-}$ (D) mice. Δ Tension was calculated as the change from baseline tension (mN) normalised to vessel length (mm) and expressed as mean±SEM. **P*<0.01 vs. control; #*P*<0.01 vs. WT; n=6-9.

Figure 5. Effects of GPR55 and α_1-AR antagonists on LPI induced vasorelaxation in isolated mesenteric arteries from WT and GPR55$^{-/-}$ mice. Arteries were contracted sub-

maximally with U46619 and then concentration response curves with the GPR55 agonist, LPI, carried out in vessels from both WT and GPR55$^{-/-}$ mice shown in (A). LPI induced vasorelaxation in the absence and presence of CID16020046 (CID) in (B) or tamsulosin in (C) in mesenteric arteries from WT mice. Relaxation was calculated as % of the maximum contraction and expressed as mean±SEM. *P<0.01 vs. WT; #P<0.01 30μM CID vs. control; †P<0.01 100μM CID vs. control; n=6-10.

Figure 6. BRET saturation experiments using CHO-K1 cells transfected with Rluc8 tagged α_{1A}-AR and Venus tagged V2R or GPR55 constructs. The presence of a saturation curve indicates α_{1A}-AR-V2R heteromerization (A), while the absence of a curve provides evidence that α_{1A}-AR and GPR55 do not dimerize (B). n=3 independent experiments.

Figure 7. Agonist induced ERK1/2 phosphorylation in CHO-K1 cells transiently transfected with tagged cDNA constructs encoding α_{1A}-AR or GPR55. A61603 induced ERK1/2 phosphorylation in CHO-K1 cells transfected with untagged or Rluc8 tagged α_{1A}-AR constructs (A). LPI induced ERK1/2 phosphorylation in CHO-K1 cells transfected with untagged or Venus tagged GPR55 constructs (B). Agonist induced ERK1/2 phosphorylation was calculated as the fold change over the vehicle control (i.e. basal phosphorylation) and expressed as mean±SEM. n=4-5 independent experiments.

Figure 8. GPCR mRNA expression in neonatal rat ventricular cardiomyocytes. Values are presented as the mean±SEM. n=5-6.

Figure 9. Agonist induced ERK1/2 phosphorylation in neonatal rat ventricular cardiomyocytes. A61603 induced ERK1/2 phosphorylation in cardiomyocytes was assessed in the absence or presence of tamsulosin in (A) or CID16020046 (CID) in

(B). LPI induced ERK1/2 phosphorylation in cardiomyocytes was assessed in both the absence and presence of tamsulosin in (C) or CID16020046 (CID) in (D). Agonist induced ERK1/2 phosphorylation was calculated as the fold change over the vehicle control (i.e. basal phosphorylation) and expressed as mean±SEM. *P<0.05 vs. control; Each data point reflects the average of 3 replicates per plate from 3-7 independent experiments.

Figure 1

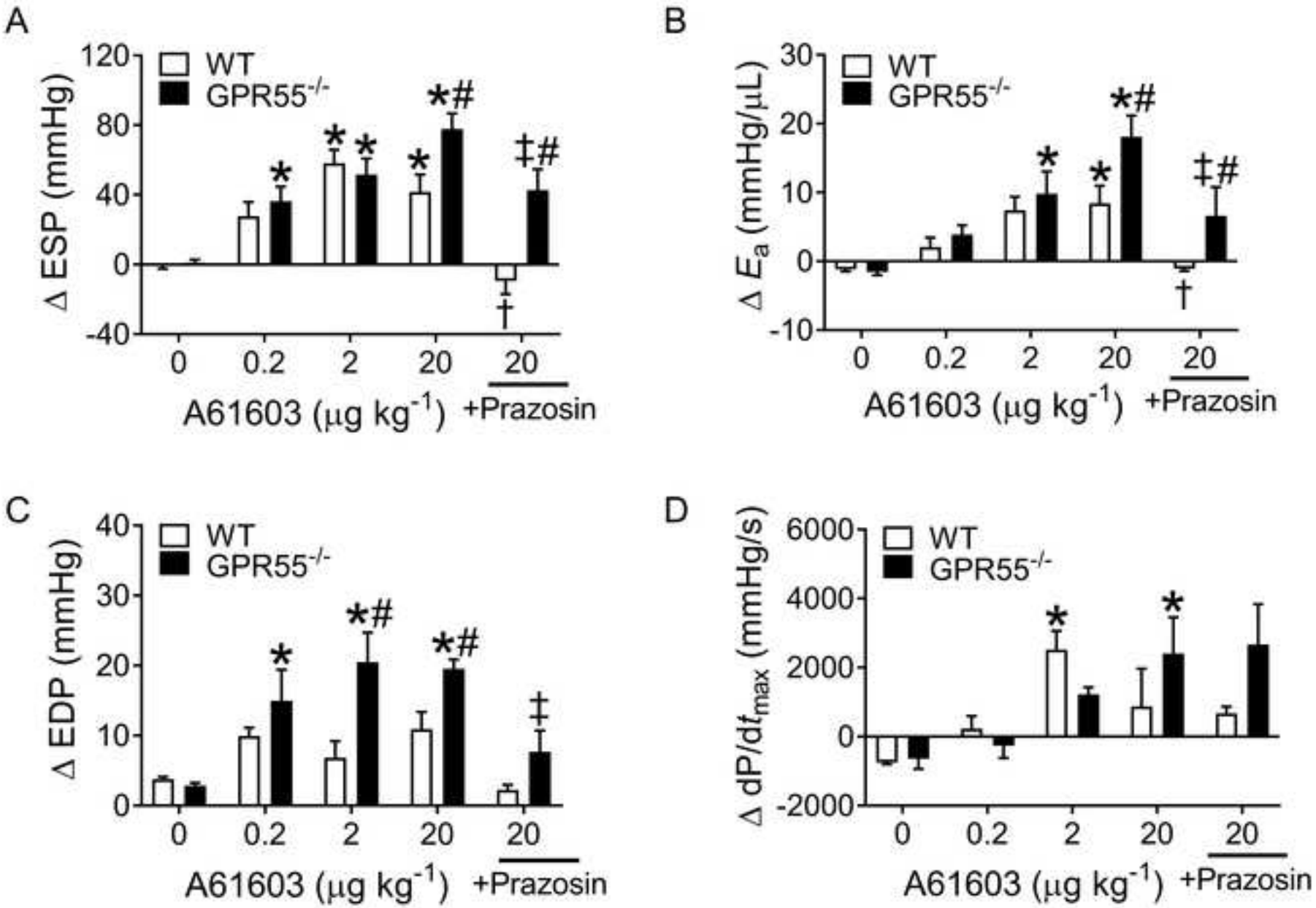

Figure 2

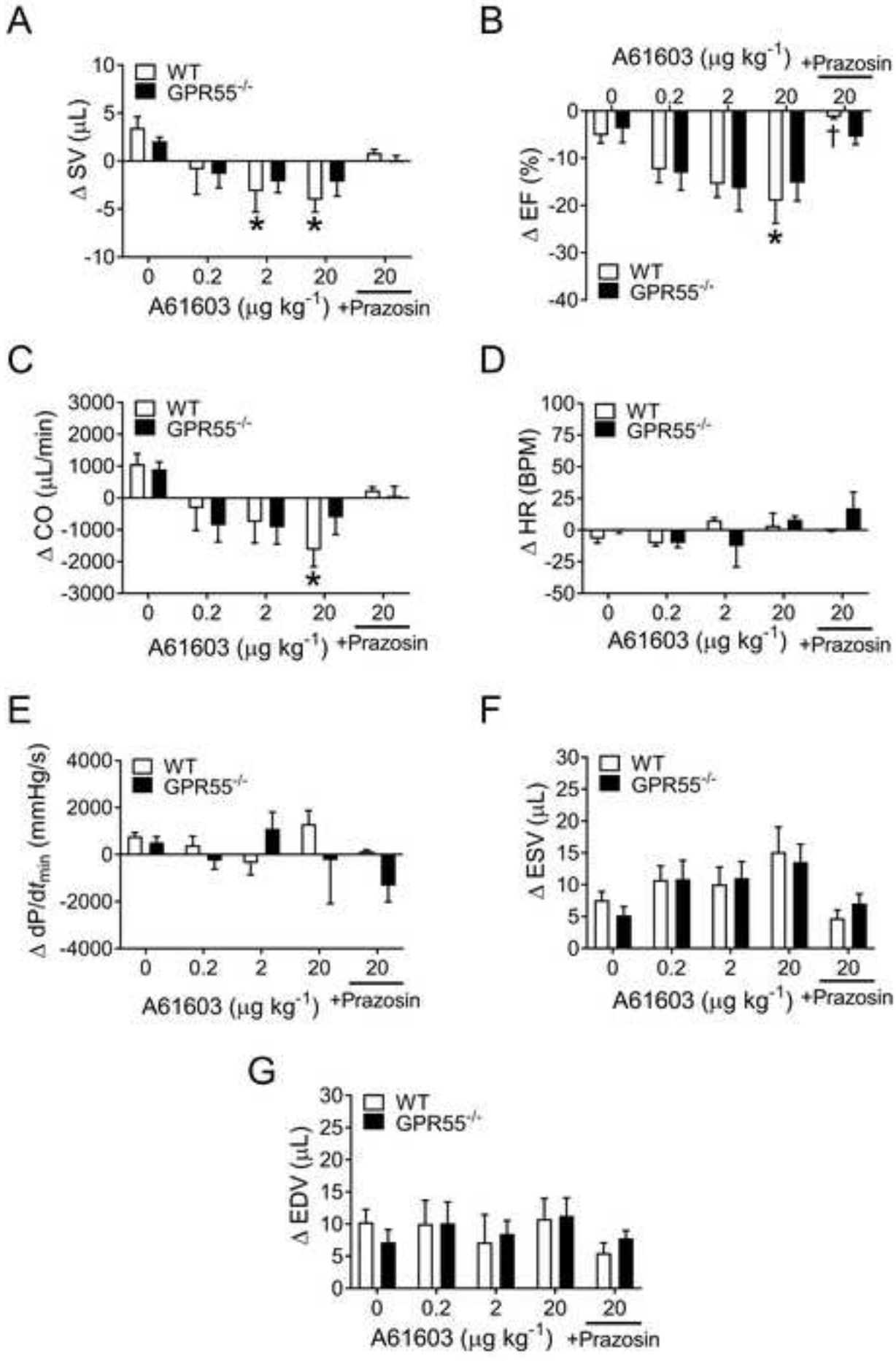

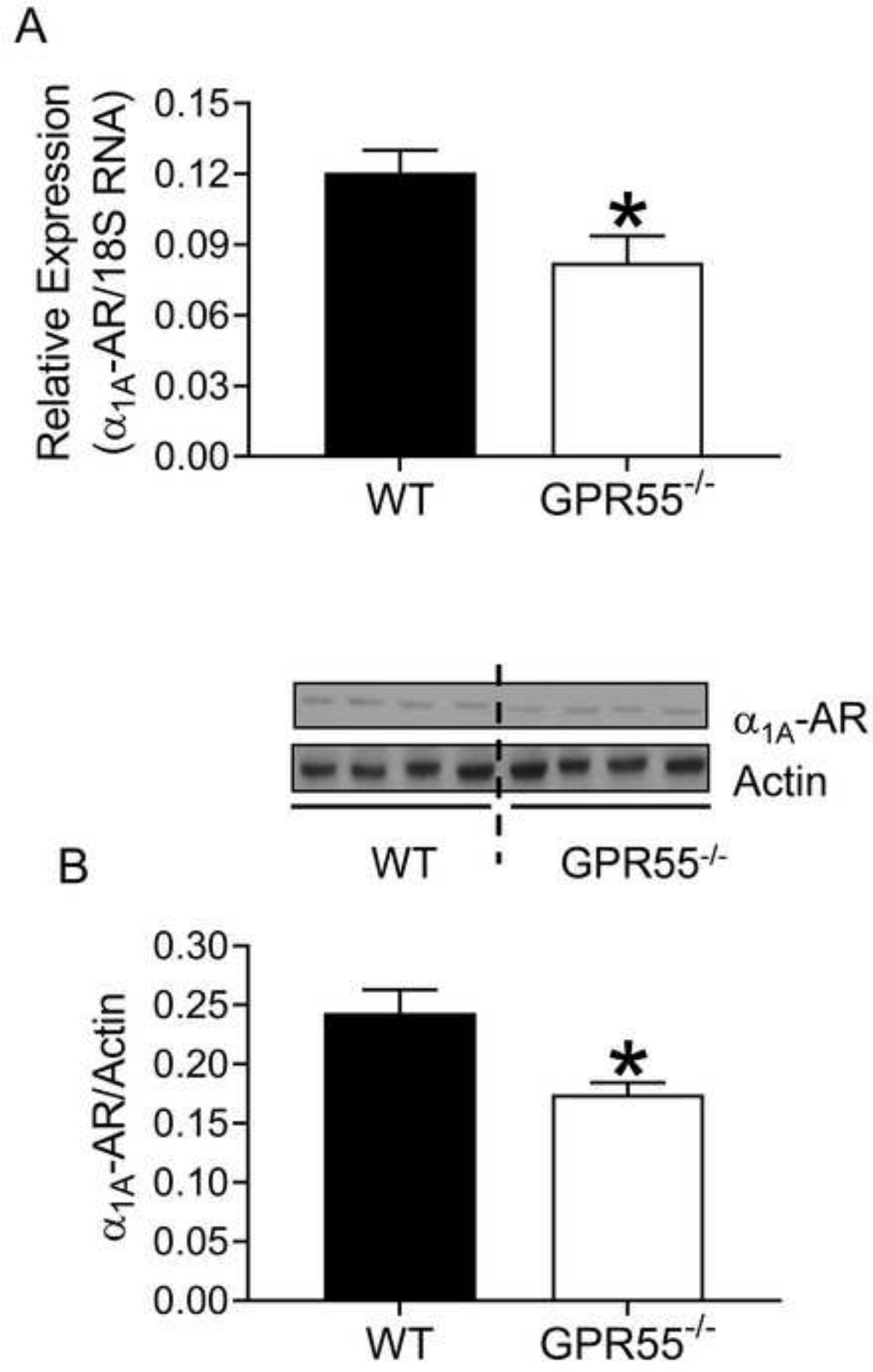

Figure 4

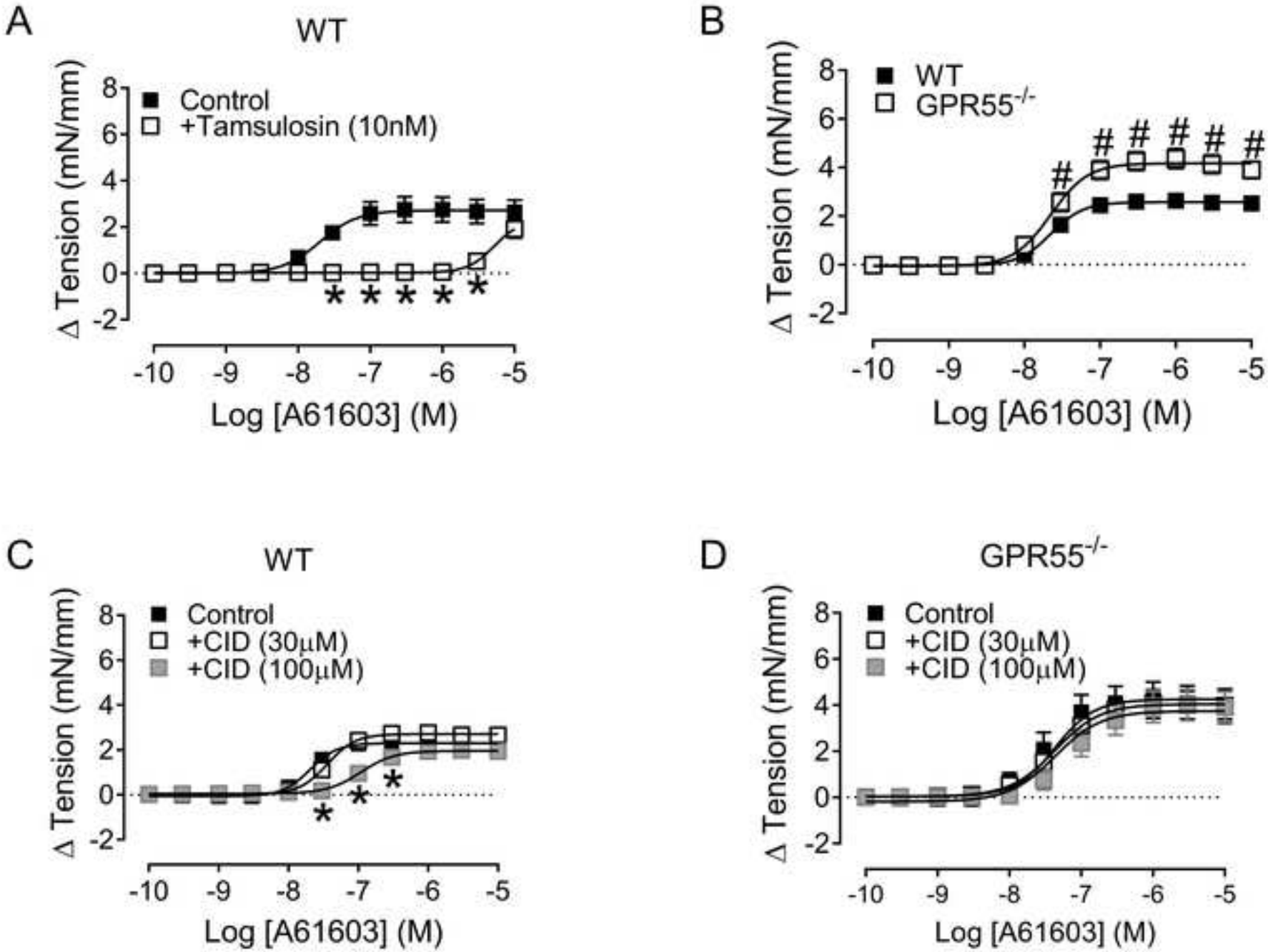

Figure 5

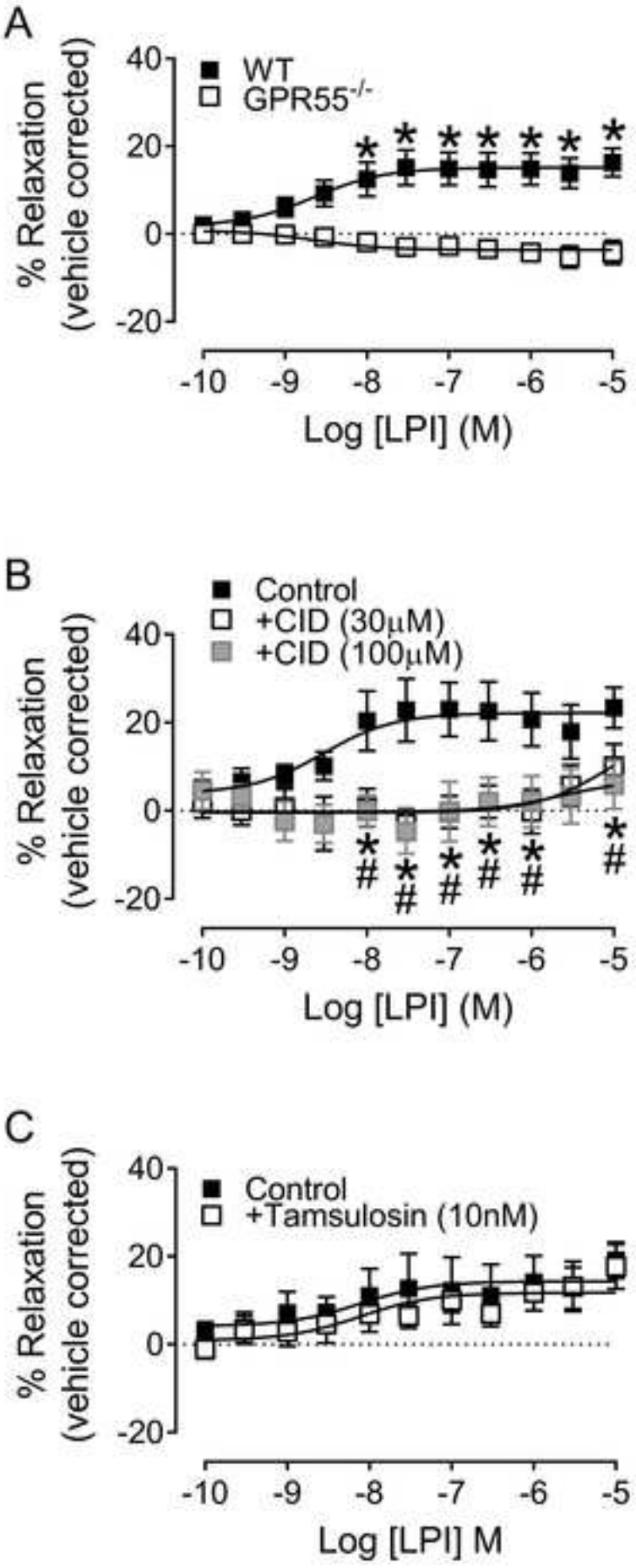

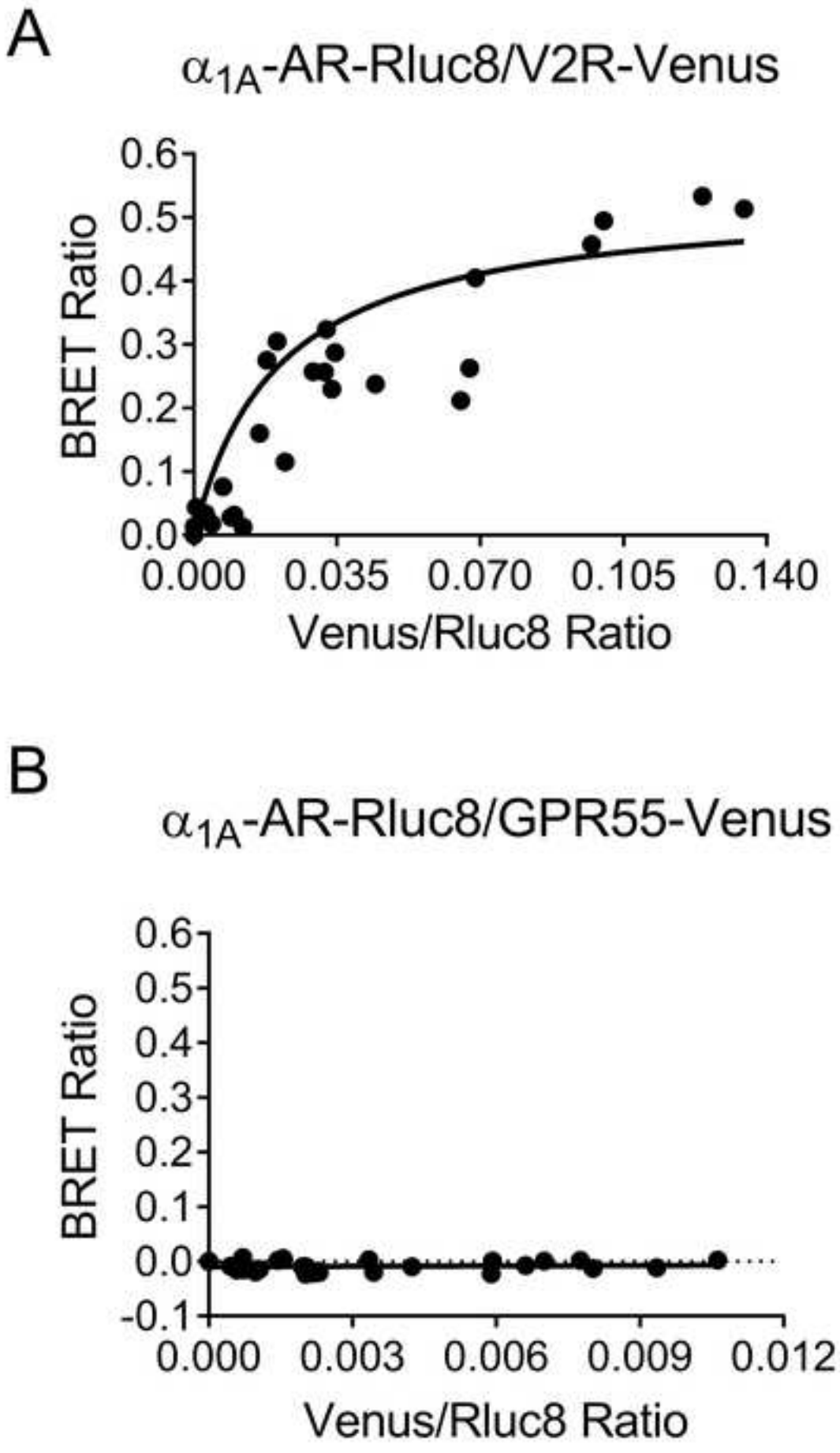

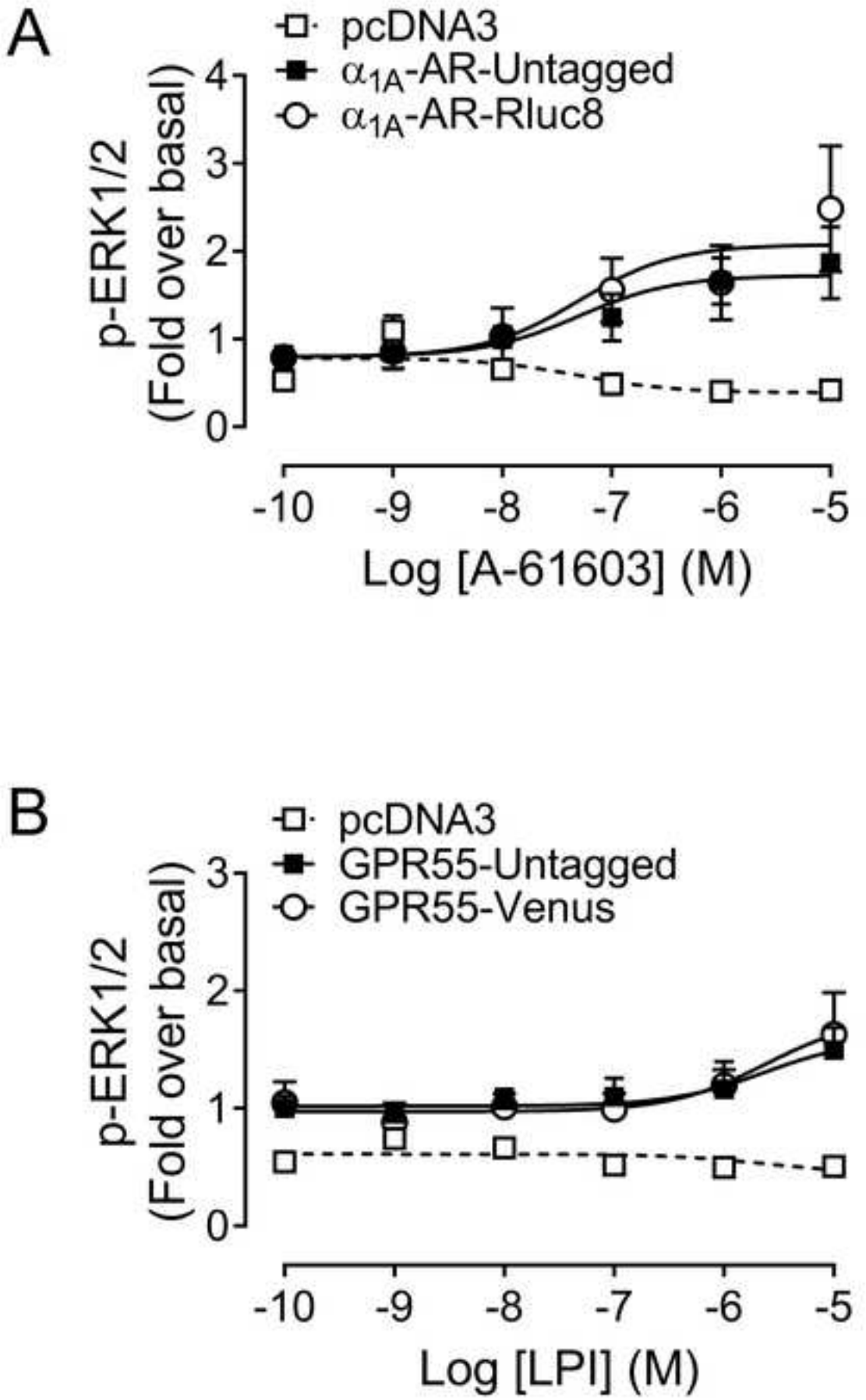

Figure 8

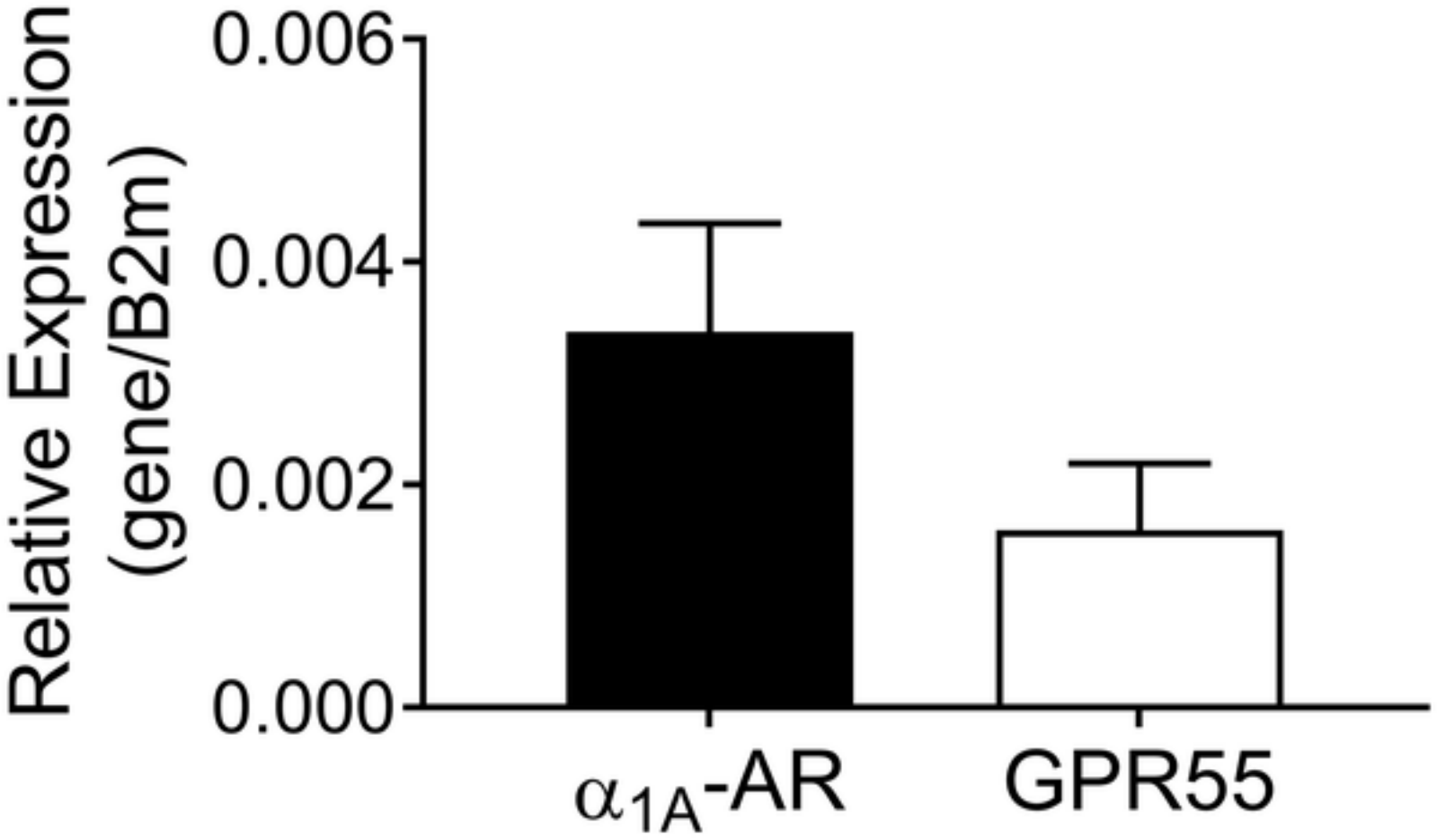

Figure 9

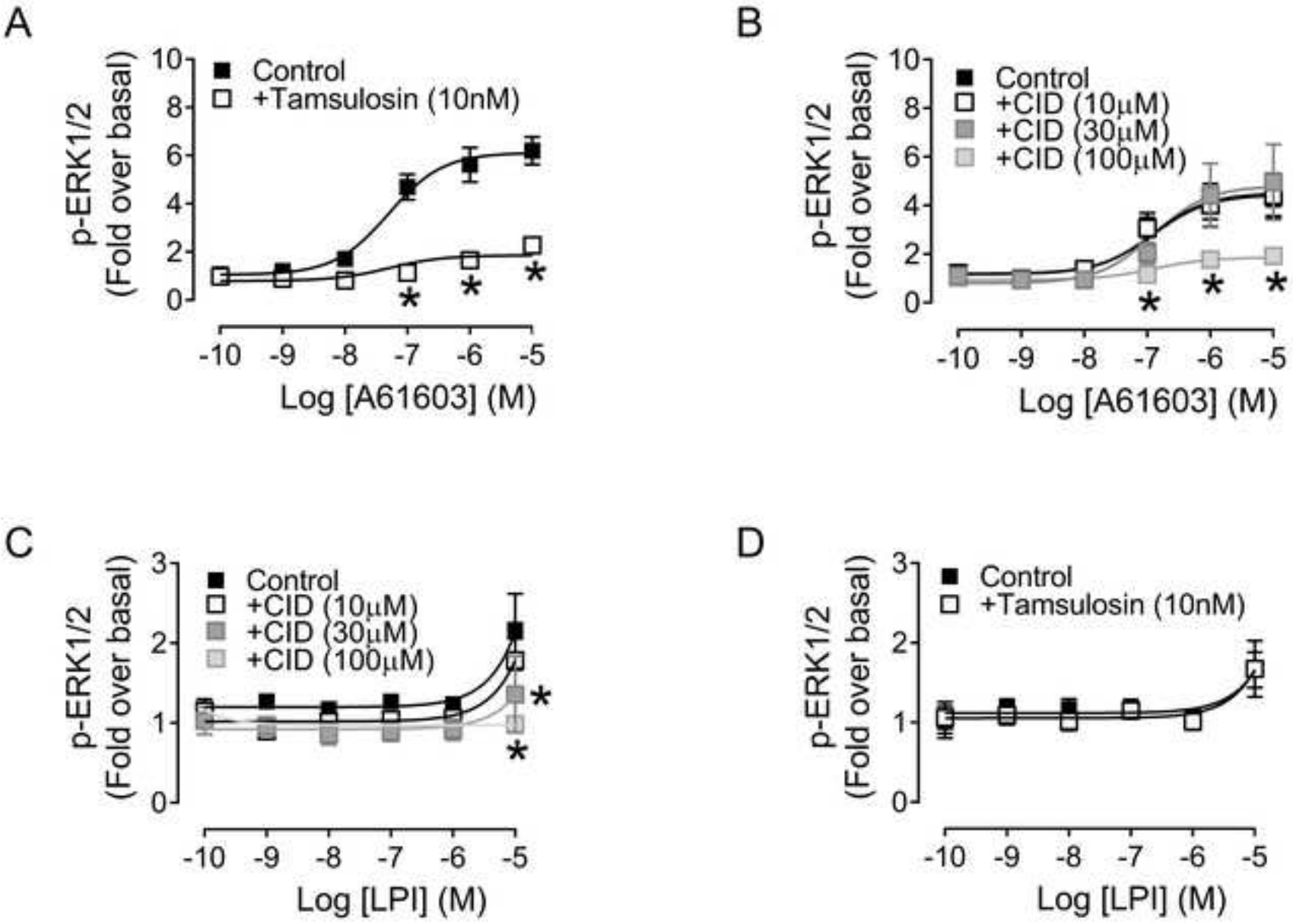

	WT (n=17)	GPR55$^{-/-}$ (n=9)
Body weight (g)	29±0.5	28±0.5
HW:BW (mg/g)	4.57±0.1	4.78±0.1
HR (bpm)	393±10	**446±21***
MABP (mmHg)	91.1±2.8	**104.2±1.6***
SBP (mmHg)	111.1±2.8	**129.5±3.1***
DBP (mmHg)	82.4±3.1	88.2±2.5
ESP (mmHg)	98.1±2.5	105.2±2.9
EDP (mmHg)	5.7±0.5	4.8±0.4
ESV (µL)	15±0.8	13.2±0.8
EDV (µL)	31.7±1.5	29.1±1.1
SV (µL)	16.7±0.5	16.6±0.9
SW (mmHg*µL)	1263±61	1154±54
CO (µL/min)	6716±198	6941±529
E_a (mmHg/µL)	7.3±0.3	8.2±0.6
EF (%)	53.8±1.1	57.1±1.8
dP/dt_{max} (mmHg/s)	8142±302	8559±731
dP/dt_{min} (mmHg/s)	-8043±417	-8361±568

Table I. Baseline cardiac function in WT and GPR55$^{-/-}$ mice. Deletion of GPR55 in mice lead to elevated blood pressure and heart rate compared to WT mice. Data is expressed as mean±SEM. *P<0.01 vs. WT.

Δ from baseline cardiac function	LPI (µg kg^{-1})			
	0	10	30	100
HR (BPM)	-3±7	-7±3	-7±2	-6±3
ESP (mmHg)	0.6±4.9	-5.3±3.9	-3.1±2.7	-4.1±2.9
EDP (mmHg)	5.3±0.7	4.3±0.7	3.1±1	4±0.6
ESV (µL)	8.4±1.1	8.2±0.9	7.8±0.9	7.5±0.7
EDV (µL)	8.3±1.4	8.1±1	7.2±1	6.9±0.6
SV (µL)	0.7±0.8	1.1±0.4	1.3±0.4	0.8±0.3
CO (µL/min)	224±349	373±162	424±161	164±153
E_a (mmHg/µL)	-0.2±0.6	-0.5±0.6	-0.9±0.5	-0.5±0.4
EF (%)	-8.7±1.8	-6.9±1.1	-5±0.6	-4.9±0.8
dP/dt_{max} (mmHg/s)	-573±340	-1191±296	-663±385	-910±326
dP/dt_{min} (mmHg/s)	758±172	957±319	852±325	1273±215

Table II. Effect of increasing doses of LPI (GPR55 agonist) on cardiac function in WT mice. The Δ from baseline cardiac function induced by LPI (10-100µg kg^{-1}) was calculated and data expressed as mean±SEM. n=8.

A61603 induced ERK1/2 phosphorylation	Maximal fold over basal
DMEM (n=7)	6.20±0.58
Tamsulosin (10nM) (n=6)	**2.27±0.12***
0.1% DMSO (n=7)	4.24±0.67
CID16020046 (10μM) (n=7)	4.40±0.91
CID16020046 (30μM) (n=7)	4.96±1.56
CID16020046 (100μM) (n=3)	**1.92±0.08#**
LPI induced ERK1/2 phosphorylation	**Maximal fold over basal**
DMEM (n=7)	1.55±0.22
Tamsulosin (10nM) (n=7)	1.49±0.32
0.1% DMSO (n=7)	2.14±0.48
CID16020046 (10μM) (n=7)	1.79±0.47
CID16020046 (30μM) (n=7)	**1.36±0.48#**
CID16020046 (100μM) (n=3)	**0.98±0.06#**

Table III. Effects of GPR55 and α_1-AR antagonists on both LPI and A61603 induced ERK1/2 phosphorylation in rat neonatal ventricular cardiomyocytes. Maximal fold change values for LPI and A61603 induced ERK1/2 phosphorylation in the absence and presence of either tamsulosin or CID16020046. All data is expressed as mean±SEM. *P<0.05 vs. DMEM; #P<0.05 vs. DMEM (0.1% DMSO).